4668 J. Med. Chem. 2009, 52, 4668–4682
DOI: 10.1021/jm801599a

Journal of Medicinal Chemistry Article

Synthesis, in Vivo Evaluation, and Molecular Modeling Studies of New Pyrazolo[5,1-*c*][1,2,4]benzotriazine 5-Oxide Derivatives. Identification of a Bifunctional Hydrogen Bond Area Related to the Inverse Agonism

Gabriella Guerrini,*[,†] Giovanna Ciciani,[†] Giovanni Cambi,[†] Fabrizio Bruni,[†] Silvia Selleri,[†] Chiara Guarino,[†] Fabrizio Melani,[‡] Marina Montali,[§] Claudia Martini,[§] Carla Ghelardini,[∥] Monica Norcini,[∥] and Annarella Costanzo[†]

[†]*Dipartimento di Scienze Farmaceutiche, Laboratorio di Progettazione, Sintesi e Studio di Eterocicli Biologicamente attivi (HeteroBioLab), Università degli Studi di Firenze, Via U. Schiff 6, 50019 Polo Scientifico, Sesto Fiorentino−Firenze, Italy,* [‡]*Dipartimento di Scienze Farmaceutiche, Laboratorio di Molecular Modeling, Cheminformatics and QSAR, Università degli Studi di Firenze, Via U. Schiff 6, 50019 Polo Scientifico, Sesto Fiorentino−Firenze, Italy,* [§]*Dipartimento di Psichiatria, Neurobiologia, Farmacologia e Biotecnologie, Università degli Studi di Pisa, via Bonanno 6, 56126 Pisa, Italy, and* [∥]*Dipartimento di Farmacologia Preclinica e Clinica Aiazzi-Mancini, Università degli Studi di Firenze, Viale Pieraccini 6, 50139 Firenze, Italy*

Received December 18, 2008

A new series of pyrazolo[5,1-*c*][1,2,4]benzotriazine 5-oxide 8-alkyloxy-/aryloxy-/arylalkyloxy and 8-aryl-/arylalkylderivatives variously substituted at the 3-position were synthesized and binding studies at the benzodiazepine site on $GABA_A$ receptor were carried out. The pharmacological profile was identified for compounds **10**, **11**, **16**(+), **16**(−), and **17** by considering six potential benzodiazepine actions: motor coordination, anticonvulsant action, spontaneous motility and explorative activity, potential anxiolytic-like effects, mouse learning and memory modulation, and finally, ethanol-potentiating action. Compound **17** stands out as the compound that improves mouse memory processes selectively, safely, and in a statistically significant manner. From a ligand-based pharmacophoric model, we identified a hydrogen bond interaction area HBp-3 near the lipophilic area. This new pharmacophoric model allowed us to identify four structural compound typologies and thus to rationalize the affinity data of all compounds.

Introduction

Ionotropic GABA receptors ($GABA_A$[a]), like other members of the ligand-gated ion channels (LGICs) superfamily, are considered to be heteropentamers composed of five protein subunits arranged to form a central ion channel. A total of 19 protein subunits, encoded by different genes, are grouped into isoforms $\alpha_{(1-6)}$, $\beta_{(1-3)}$, $\gamma_{(1-3)}$, δ, ε, π, θ, and $\rho_{(1-3)}$ and have been cloned and sequenced from the mammalian nervous system. Despite the great repertoire of $GABA_A$ receptors that could exist (more than 2000 different receptors), the majority of $GABA_A$ receptors expressed in the central nervous system are formed by subunits $\alpha_1\beta_2\gamma_2$ (about 60%), with $\alpha_2\beta_3\gamma_2$, $\alpha_3\beta_3\gamma_2$ also prevalent (15−20%), assembled in 2:2:1 stoichiometry. The other assembled $GABA_A$ receptor subunits ($\alpha_{4-6}\beta_n\gamma_n$) are less abundant (about 5%) and with confined distributions. For example, receptors containing the α_5 isoform are localized in the hippocampus, olfactory bulb, and hypothalamus and are extra synaptic receptors. The α_4 isoform, whose distribution parallels that of δ subunit, is localized in the thalamus and hippocampus basal ganglia and forms extra synaptic receptors.[1−4] Benzodiazepines (Bzs), which bind the $GABA_A$ receptor at the interface of the α and γ subunit, are known to be positive allosteric modulators at only a subset of $GABA_A$ receptors: α_1-, α_2-, α_3-, and α_5-containing receptors, respectively. However, different classes of compounds, the nonbenzodiazepine ligands, can interact with the benzodiazepine binding site, acting with different profiles (agonist, antagonist, and inverse agonist) and subtype affinities than the benzodiazepines.[3,5−7] In an attempt to link distinct pharmacological functions with certain $GABA_A$ receptor subtypes, genetic and medicinal chemistry approaches have been used by researchers.[8] The genetic approach utilizes transgenic mice with point mutation on the α subunit while the chemistry approach synthesizes ligands endowed with selective affinity or efficacy. These approaches help to explain the important role of $\alpha_{(1-3,\,5)}$-isoform on drugs action. It has been proposed that the α_1-subunits mediate sedation and that they could be the target for sedative−hypnotic agents. Agonists at α_2- and/or α_3-containing $GABA_A$ receptors have been shown to provide anxiolysis. Inverse agonists at the α_5-isoform could be useful for memory enhancement because these extra synaptic receptors, mainly localized in the hippocampus, play a key role in cognitive processes.[1,6−17] An interesting new potential role for α_3- and α_5-selective agonists has been demonstrated. In particular,

*To whom correspondence should be addressed. Phone: +39-055-4573766. Fax: +39-055-4573671. E-mail: gabriella.guerrini@unifi.it.

[a] Abbreviations: $GABA_A$, GABA type A receptor; LGCIs, ligand-gated ion channels; Bzs, benzodiazepines; SAR, structure−affinity relationships; $Bu_4N^+Br^-$, tetrabutylammonium bromide; $Pd(PPh_3)_4$, tetrakis(triphenylphosphine)palladium(0); $PdCl_2(dppf)CH_2Cl_2$, [1,1′-bis(diphenyl phosphino)ferrocene]palladium(II)chloride; PTZ, pentylenetetrazole; Pp, pharmacophoric point; Lp, lipophilic point; HBp, hydrogen bond interaction point; CGS 9896, 2-(4-chlorophenyl) pyrazolo[4,3-*c*]quinolin-3-one; Diazepam: 7-chloro-1-methyl-5-phenyl-3*H*-1,4-benzodiazepin-2(1*H*)-one.

 Published on Web 07/10/2009

Chart 1

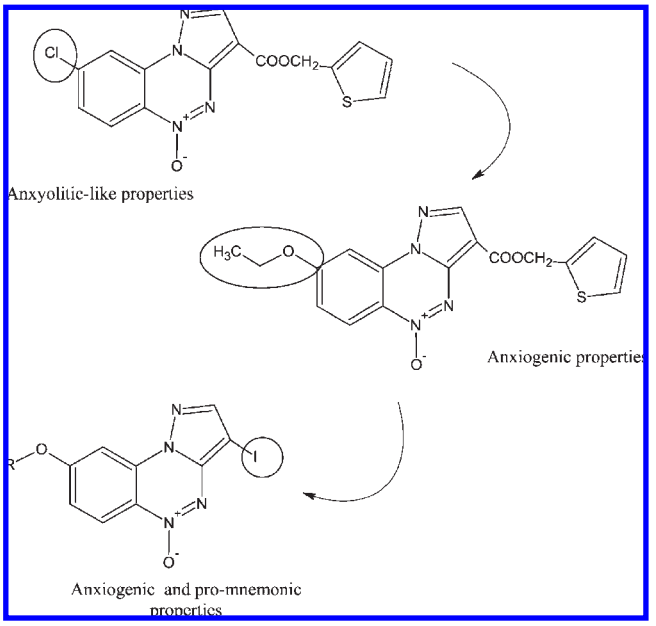

α_3-containing $GABA_A$ receptors represent the main inhibitory input for the dopaminergic system,[18] whose hyperfunction appears to be typical of various psychiatric disorders.[8,19] Moreover, it has been observed that point-mutated mice α_5(H101R), or mice with a partial loss of the α_5-containing $GABA_A$ receptors, exhibit an increase of spontaneous locomotor activity, a typical sensorimotor dysfunction associated with psychiatric disorders.[2,16,20] Thus, it is plausible that a full agonist at α_3- and α_5-containing $GABA_A$ receptors may be useful in various psychiatric conditions.[21]

In the attempt to obtain compounds endowed with more selective affinity or selective efficacy for a subtype of the $GABA_A$ receptor, we focused on position 8 of the pyrazolo-[5,1-*c*][1,2,4]benzotriazine system, whose chemical modulation allowed us to obtain different pharmacological effects. We recently reported that, within the pyrazolo[5,1-*c*]-[1,2,4]benzotriazine series, the different lipophilic, steric, and electronic features of the 8-substituent seem to influence the in vivo efficacy of ligands. Our research was particularly intriguing in that the simple substitution of the chlorine atom (σ = 0.23) at position 8 with an ethoxy group (σ = −0.24)[22] brought about an overturning of the in vivo profile from agonist to inverse agonist. The 8-chloroderivative showed selective anxiolytic-like activity, and the 8-ethoxy derivative showed selective anxiogenic properties (see Chart 1).[23−26] It was later demonstrated that the introduction of an iodine atom, at position 3 on the 8-alkyloxypyrazolo[5,1-*c*][1,2,4]benzotriazine core, provided ligands endowed with anxiogenic and pro-mnemonic properties,[25,26] enlarging efficacy spectrum (see Chart 1). The best compound in terms of affinity value (K_i = 0.8 nM) was the 8-propinyloxy derivative. In this case, it was suggested that the presence of the triple bond, capable of forming a $\pi-\pi$ stacking interaction, was responsible for this high receptor affinity.

Thus we focused our research on the evaluation of the size, steric and stereochemical features of the 8-O-substituent to obtain the pro-mnemonic profile only. A series of new 3-iodo-8-alkyloxy-/aryloxy-/arylalkyloxyderivatives (**8**−**23**, 5-*N*-oxides and **11R**, 5-*N*-deoxide) was prepared and biological assays were carried out.

The synthesis and biological investigation of derivatives **24**−**30**, variously substituted at position 3, were carried out to understand the interdependence, if any, between positions 3 and 8.

The next step, to better explore the role of the oxygen at position 8, was the synthesis of 8-aryl-/arylalkylderivatives variously substituted at the 3-position, **33**, **36**−**39**, **41**, and **42**. The 8-substitutent was, however, able to form a $\pi-\pi$ stacking interaction with the receptor protein and the removal of the oxygen atom eliminated the possibility of engaging a hydrogen bond as previously evidenced.[27] At this point, we were able to evaluate the actual driving force of binding of 3-derivatives.

Finally, we performed an in-depth molecular modeling study to generate a ligand-based pharmacophoric model with the aim of correlating the binding and in vivo data and increasing our knowledge about the requirements of the Bzs site of the $GABA_A$ receptor.

Chemistry

All compounds described here are listed in Table 1 (chemical data).

The starting material for the synthesis of 8-alkyloxy-, 8-aryloxy-, and 8-arylalkyloxypyrazolo[5,1-*c*][1,2,4]benzotriazine 5-oxides variously substituted at the 3-position, **8**−**30**, were the corresponding 3-iodo-, **1**,[26,28] 3-chloro-, **2**,[26] 3-thienyl-, **3**,[23] 3-ethoxycarbonyl-, **4**,[29] 3-(2-thienylmethoxycarbonyl)-, **5**,[24] 3-(2-methoxybenzyloxycarbonyl)-, **6**,[24] and 3-unsubstituted-8-chloropyrazolo[5,1-*c*][1,2,4] benzotriazine 5-oxides **7**.[29]

The nucleophilic substitution at position 8 of the benzotriazine system occurred by phase transfer catalyzed (PTC)[30] chlorine displacement. In this procedure, the suitable alcohol is added to a two-phase system consisting of a strong aqueous sodium hydroxide solution (40%), catalyst (tetrabutylammonium bromide, $Bu_4N^+Br^-$), and a methylene chloride solution of starting material (see Scheme 1).

Compounds **33**−**36**, the 8-arylderivatives, were achieved using Suzuki cross-coupling (Scheme 2). In particular, **31**[26] and **32**[25] were reacted with suitable boronic acids, using tetrakis (triphenylphosphine) palladium(0) ($Pd(PPh_3)_4$) as a catalyst, to obtain compounds **33**, **35**, and **36** and [1,1′-bis(diphenylphosphino)ferrocene]palladium(II)chloride complex with dichloromethane ($PdCl_2$(dppf) CH_2Cl_2)[31] for compound **34**.

Halogenation in position 3 was the second step to obtaining the final desired compounds **37**−**39**, **41**−**42**. Compounds **37**−**38** were obtained starting from **33**−**34**, which were iodinated by $ICl/CHCl_3$.

A particular reactivity in the presence of $ICl/CHCl_3$ was observed for **35**: this compound underwent a double-halo addition at the double bond, as well as the 3-iodination and the product 3-iodo-8-(1-chloro-2-iodo-2-phenylethyl)pyrazolo[5,1-*c*][1,2,4]benzotriazine 5-oxide (**40**) was recovered after purification of the reaction mixture. This mixture, from ^1H NMR spectra, was made up of **40** and its isomer 3-iodo-8-(1-iodo-2-chloro-2-phenylethyl)pyrazolo[5,1-*c*][1,2,4]benzotriazine 5-oxide in 10:1 ratio. The iodination of **35** by $NIS/CHCl_3$ gave the desired compound **39**. Compounds **41** and **42** were synthesized starting from **33**, using $NCS/CHCl_3$ and $Br_2/CHCl_3$.

Compound **11** was deoxidized at position 5 with triethylphosphite/toluene to obtain compound **11R**.

Biological Results

The $GABA_A$/BzR complex binding affinity of new 3-substituted-8-alkyloxy-/aryloxy-/arylalkyloxyderivatives (**8**−**30**,

Table 1. Chemical Data for New Synthesized Compounds (**8**−**42**)

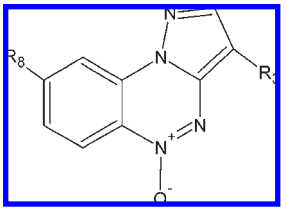

no.	R_3	R_8	MF (MW)	Yield (%)	mp °C (recrystallized solvent)
8	I	$O(CH_2)_7CH_3$	$C_{17}H_{21}O_2N_4I$ (440.29)	68	118−119 (ethanol)
9	I	OC_6H_{11}	$C_{15}H_{15}O_2N_4I$ (410.20)	40	206−207 (ethanol)
10	I	OPh	$C_{15}H_9O_2N_4I$ (404.16)	86	245−246 (ethanol)
11	I	OCH_2Ph	$C_{16}H_{11}O_2N_4I$ (418.18)	50	219−220 (*i*-propyl alcohol)
11R[a]	I	OCH_2Ph	$C_{16}H_{11}ON_4I$ (402.18)	69	188−189 (ethanol)
12	I	OCH_2-*o*-OCH_3Ph	$C_{17}H_{13}O_3N_4I$ (448.22)	55	219−220 (methoxyethanol)
13	I	OCH_2-*p*-OCH_3Ph	$C_{17}H_{13}O_3N_4I$ (448.22)	40	148−149 (ethanol)
14	I	OCH_2-*o*-OCF_3Ph	$C_{17}H_{10}O_3N_4IF_3$ (502.2)	65	194−196 (ethanol)
15	I	OCH_2-*p*-ClPh	$C_{16}H_{10}O_2N_4ICl$(452.64)	60	256−257 (ethanol)
16(±)	I	$OCH(CH_3)Ph$	$C_{17}H_{13}O_2N_4I$ (432.2)	80	210−211 (ethanol)
16(+)	I	$OCH(CH_3)Ph$	$C_{17}H_{13}O_2N_4I$ (432.2)	48	185−186 (ethanol)
16(−)	I	$OCH(CH_3)Ph$	$C_{17}H_{13}O_2N_4I$ (432.2)	40	185−186 (ethanol)
17	I	OCH_2-4-Py	$C_{15}H_{10}O_2N_5I$ (419.17)	60	229−230 (methoxyethanol)
18	I	OCH_2-2-thienyl	$C_{14}H_9O_2N_4IS$ (424.15)	75	196−198 (ethanol)
19	I	OCH_2-2-furyl	$C_{14}H_9O_3N_4I$ (408.52)	75	204−206 (ethanol)
20	I	OCH_2CH_2Ph	$C_{17}H_{13}O_2N_4I$ (432.21)	49	161−162 (*i*-propyl alcohol)
21	I	$OCH(CH_3)CH_2Ph$	$C_{18}H_{15}O_2N_4I$ (446.25)	60	178−179 (ethanol)
22	I	$OCH_2CH(CH_3)$ Ph	$C_{18}H_{15}O_2N_4I$ (446.25)	72	175−176 (ethanol)
23	I	O-2-naphthyl	$C_{19}H_{11}O_2N_4I$ (453.9)	35	>300 (chrom. column)[b]
24	Cl	OPh	$C_{15}H_9O_2N_4Cl$ (312.72)	51	191−192 (ethanol)
25	3-thienyl	OPh	$C_{19}H_{12}O_2N_4S$ (360.40)	45	218−219 (ethanol)
26	$COOCH_2CH_3$	OPh	$C_{18}H_{14}O_4N_4$ (350.34)	45	207−208 (ethanol)
27	$COOCH_2$-2-thienyl	OPh	$C_{21}H_{14}O_4N_4S$ (418.20)	62	213−215 (ethanol)
28	$COOCH_2$-*o*-OMePh	OPh	$C_{24}H_{18}O_5N_4$ (442.43)	35	187−188 (*i*-propyl alcohol)
29	H	OCH_2Ph	$C_{16}H_{12}O_2N_4$ (292.5)	47	174−175 (ethanol)
30	$COOCH_2CH_3$	OCH_2Ph	$C_{19}H_{16}O_4N_4$ (364.40)	25	156−158 (chrom. column)[b]
33	H	Ph	$C_{15}H_{10}ON_4$ (262.16)	60	176−177 (ethanol)
34	H	CH_2CH_2Ph	$C_{17}H_{14}ON_4$ (290.18)	22	199−200 (chrom. column)[b]
35	H	CH=CH-Ph	$C_{17}H_{12}ON_4$ (288.29)	35	181−182 (ethanol)
36	COOEt	Ph	$C_{18}H_{14}O_3N_4$ (334.34)	73	206−207 (ethanol)
37	I	Ph	$C_{15}H_9ON_4I$ (388.17)	95	220−221 (ethanol)
28	I	CH_2CH_2Ph	$C_{17}H_{13}ON_4I$ (416.21)	18	290−291 (ethanol)
39	I	CH=CH-Ph	$C_{17}H_{11}ON_4I$ (414.19)	32	245−246 (*i*-propyl alcohol)
40	I	CHCl-CHI-Ph	$C_{17}H_{11}ON_4ClI_2$ (576.55)	28	199−200 (ethanol 80%)
41	Cl	Ph	$C_{15}H_9ON_4Cl$ (296.72)	60	178−179 (ethanol)
42	Br	Ph	$C_{15}H_9ON_4Br$ (341.08)	80	188−190 (ethanol)

[a] 5-Deoxide derivative. [b] Eluent: chloroform for compound **23**, toluene/ethyl acetate/acetic acid 8:2:1 for compound **30**, and toluene/ethyl acetate 8:2 for compound **34**.

11R) and 8-aryl-/arylalkylderivatives (**33**, **36**−**39**, **41**, and **42**) was evaluated by their ability to displace [^{3}H]flumazenil (Ro15-1788) from its specific binding in bovine brain membrane.[28] The affinity was expressed as K_i value only for those compounds inhibiting radioligand binding by more than 80% at fixed concentrations of 10 μM. Binding data are reported in Table 2.

To explore the size and shape of the pocket in which the 8-substituent fits, a further extension and conformational restriction was carried out with the synthesis of the new derivatives, 3-iodo-8-octyloxy- and 3-iodo-8-cyclohexyloxypyrazolo[5,1-*c*][1,2,4]benzotriazine 5-oxides, **8** and **9**, respectively (Table 2). The lengthening of the alkyloxy chain by up to eight carbon atoms, as in **8**, which could also confer a higher lipophilicity (8-$O(CH_2)_7CH_3$ ClogP 5.58 ± 1.35), is detrimental for receptor affinity (K_i = 1616 ± 161 nM). The insertion of the 8-cyclohexyloxy residue, as in compound **9**, which is conformationally more stable than the linear alkyloxy chain, shows an affinity value of K_i = 188 ± 18 nM.

When the cyclohexyloxy group was substituted by a phenoxy group, as in **10**, a good affinity value resulted (K_i = 8.6 ± 0.8 nM), confirming the importance of a $\pi-\pi$ system for the receptor interaction as previously reported.[26] When the iodine atom at position 3 of the 3-iodo-8-phenoxypyrazolo[5,1-*c*]-[1,2,4]benzotriazine 5-oxide (**10**) was substituted with a chlorine atom, **24**, an affinity value, reduced by about 5-fold (**24**, K_i = 43 ± 4.0 nM vs **10**, K_i = 8.6 ± 0.8 nM), was observed.

When the 8-phenoxypyrazolo[5,1-*c*][1,2,4]benzotriazine 5-oxide core was substituted at the 3-position with an ester group (3-ethoxycarbonyl-, **26**, 3-(2-thienylmethoxycarbonyl)-**27**, 3-(2-methoxyphenylmethoxycarbonyl)- **28**) a shift of affinity value toward subnanomolar range was observed:

Scheme 1[a]

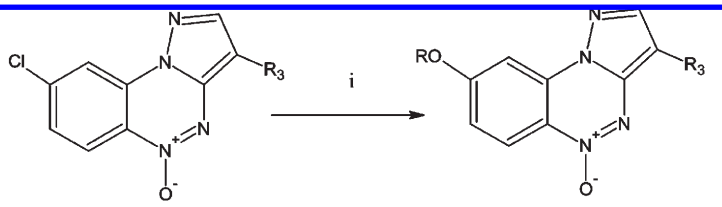

[a]Reagent and conditions:
(i)ROH/NaOH 40% solution/$NBu_4^+Br^-/CH_2Cl_2$.

1 R_3=I [28]
2 R_3= Cl [26]
3 R_3= 3-thienyl [23]
4 R_3= COOEt [29]
5 R_3= $COOCH_2$-2-thienyl [24]
6 R_3= $COOCH_2$-(2-MeO)phenyl [24]
7 R_3= H [29]

Compds	R_3	R
8	I	C_8H_{17}
9	I	C_6H_{11}
10	I	Ph
11	I	CH_2Ph
12	I	CH_2-*o*-OCH_3Ph
13	I	CH_2-*p*-OCH_3Ph
14	I	CH_2-*o*-OCF_3Ph
15	I	CH_2-*p*-ClPh
16(±)	I	(±)$CH(CH_3)Ph$
16(+)	I	(+)$CH(CH_3)Ph$
16(-)	I	(-)$CH(CH_3)Ph$
17	I	CH_2-4-Py
18	I	CH_2-2-Thienyl
19	I	CH_2-2-Furyl
20	I	CH_2CH_2Ph
21(±)	I	(±)$CH(CH_3)CH_2Ph$
22(±)	I	(±)$CH_2CH(CH_3)Ph$
23	I	2-naphtyl
24	Cl	Ph
25	3-thienyl	Ph
26	COOEt	Ph
27	$COOCH_2$-2-thienyl	Ph
28	$COOCH_2$-(2-MeO)phenyl	Ph
29	H	CH_2Ph
30	COOEt	CH_2Ph

[a] Reagent and conditions: (i) ROH/NaOH 40% solution/$NBu_4^+Br^-/CH_2Cl_2$.

$K_i = 12 \pm 1.1$ nM, 0.7 ± 0.06 nM, and 1.75 ± 0.15 nM, respectively. For these compounds, it may be hypothesized that the carbonyl group of the ester chain can reinforce the receptor binding by means of a three-centered hydrogen bond (N4/H1/CO).[24,32] Instead, the presence at position 3 of a 3-thienyl ring, as in compound **25**, gave a ligand with reduced affinity ($K_i = 68 \pm 6.5$ nM) because it lacks the hypothesized hydrogen bond.

It is noteworthy that elimination of the 8-oxygen atom of the phenoxy group, as in compounds **33**, **36**, **37**, **41**, and **42**, compared to compounds **10**, **24**, and **26**, drastically reduces (compounds **37**, $K_i = 966 \pm 95$ nM, **42**, $K_i = 802 \pm 75$ nM) or cancels the binding (compounds **33**, **36**, and **41**).

The 3-iodo-8-benzyloxypyrazolo[5,1-*c*][1,2,4]benzotriazine 5-oxide, **11**, had better affinity for the 8-phenoxy derivative, **10**, (**11**, $K_i = 1.1 \pm 0.1$ nM vs **10**, $K_i = 8.6 \pm 0.8$ nM). The positive influence of the 8-benzyloxy substituent was also verified when an ethoxycarbonyl group was present at the 3-position (compound **30**, $K_i = 2.1 \pm 0.20$ nM) in comparison to **26** ($K_i = 12 \pm 1.1$ nM). The importance of the 3,8-disubstitution emerged because the 3-unsubstituted compound, **29**, showed reduced affinity ($K_i = 116 \pm 11.1$ nM).

Interesting information was obtained from the 5-*N*-deoxide derivative, **11R**. This compound showed a K_i value (1.0 ± 0.1 nM) comparable to its corresponding 5-oxide derivative, **11** ($K_i = 1.1 \pm 0.1$ nM), indicating a secondary role of the *N*-oxide group in the binding. The negligible effect of this group was also evidenced in the 3-arylmethoxycarbonyl derivatives (3-aryl/heteroarylesters)[24] and in the 3-heteroaroylderivatives (3-ketoderivatives).[27] For these compounds, the presence of the 3-carbonyl group was sufficient to form a three-centered hydrogen bond and allowed anchorage on the receptor protein. In compound **11R**, 8-benzyloxy-3-iodopyrazolo[5,1-*c*][1,2,4]benzotriazine, the 3 substituent was unable to form

Scheme 2[a]

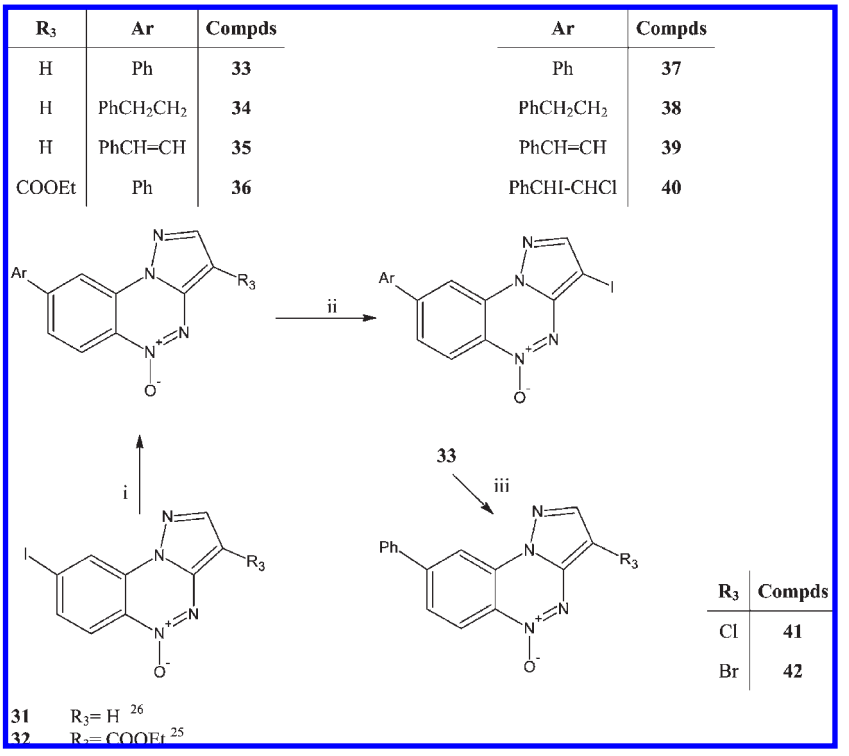

[a] Reagent and conditions: (i) Suzuki coupling: phenylboronic acid and *trans*-2-phenylvinylboronic acid, Na_2CO_3,toluene, tetrakis for **33**, **35**, and **36**; 2-phenylethylboronic acid, Na_2CO_3, THF, $PdCl_2(dppf)CH_2Cl_2$ for **34**. (ii) $ICl/CHCl_3$ for compounds **37**, **38**, and **40**; $NIS/CHCl_3$ for compounds **39**. (iii) $NCS/CHCl_3$ for compound **41** $Br_2/CHCl_3$ for compound **42**.

the hydrogen bond interaction, thus its very good binding value ($K_i = 1.0 \pm 0.1$ nM) can be explained by considering that a crucial and sufficient role in the binding was played by the 8-benzyloxy group through the oxygen atom.

The drastic reduction of affinity binding of the 8-phenethyl derivative, **38** ($K_i = 464 \pm 45$ nM), confirms the important role for interaction at the receptor protein played by the oxygen at position 8. The 8-stiryl derivative, **39**, definitively lost its receptor recognition ($K_i = 2000 \pm 200$ nM).

When the phenyl ring of the benzyloxy moiety was substituted, the best group was the methoxy-, at ortho-position, conferring a subnanomolar affinity value to compound **12** ($K_i = 0.42 \pm 0.04$ nM), about 2.5-fold greater than the unsubstituted benzyloxy group, as in **11** ($K_i = 1.1 \pm 0.1$ nM). The same methoxy-, a trifluoromethoxy group or a chlorine atom at the para-position, gave ligands **13**−**15** with good affinity, even if reduced compared to **12** (K_i range 4.5 − 11.0 nM).

Interesting information arises from analysis of the binding data of compounds **16**(±), **16**(+), **16**(−) **20**, **21**(±), and **22**(±). While the raceme compound **16**(±) (8-O-$CH(CH_3)$phenyl derivative) is endowed with a good affinity value ($K_i = 3.4 \pm 0.26$ nM), the enantiomers **16**(+) and **16**(−) are very different in terms of binding affinity, allowing us to hypothesize a potential receptor stereoselectivity; in fact, **16**(+) has about 300-fold less affinity than enantiomer **16**(−) ($K_i = 605 \pm 50.0$ nM vs $K_i = 2.1 \pm 0.1$ nM).

The lengthening of the 8-O-benzyl chain of compound **11** ($K_i = 1.1 \pm 0.1$ nM) in a linear manner, as in compound **20** (8-O-CH_2CH_2-phenyl), or in a branched manner as in compounds **21**(±) (8-O-$CH(CH_3)CH_2$phenyl) and **22**(±) (8-$OCH_2CH(CH_3)$phenyl), gave reduced binding with affinity values, respectively, of **20**, $K_i = 43 \pm 4.0$ nM, **21**(±), $K_i = 103 \pm 10.0$ nM, and **22**(±), $K_i = 160 \pm 15.0$ nM.

Interesting results were given by 8-heteroarylmethoxy derivatives **17**−**19**, all three endowed with very good affinity values: **17**, $K_i = 1.3 \pm 0.1$ nM, **18**, $K_i = 1.2 \pm 0.1$ nM, **19**, $K_i = 0.8 \pm 0.08$ nM.

Compound **19** had the best affinity value, probably due to the fact that the furyl oxygen atom and the 8-oxygen work together to make a stronger "hydrogen bond interaction" within the receptor protein. Good orientation of the furyl oxygen lone pairs is probably realized. The same trend can be easily recognized also in the 8-*o*-methoxybenzyloxy derivative, **12** ($K_i = 0.42 \pm 0.04$ nM), where the methoxyl oxygen can aid the interaction in the same manner.

Finally, the 8-(2-naphtyloxy) derivative, **23**, showed a reduced affinity value ($K_i = 94 \pm 9.0$ nM) with respect to **10** ($K_i = 8.6 \pm 0.8$ nM), probably because of a steric hindrance in the receptor interaction.

Pharmacological Results

Compounds **10**, **11**, **16**(+), **16**(−), and **17** were studied in mice in vivo for their pharmacological effects. Compounds **10**, **11**, and **17** were chosen on the basis of different hydro/lipophilic features, while **16**(+) and **16**(−) were selected to evaluate if in vitro affinity was in agreement with in vivo testing. Six potential benzodiazepine actions were considered: motor coordination was screened with the rota-rod test and the anticonvulsant action was evaluated using the new drugs against pentylenetetrazole-induced convulsions (Table 4); spontaneous motility and explorative activity with the hole-board test (Table 5); potential anxiolytic-like effects were screened using the light/dark choice test (Figure 1); mouse learning and memory modulation were evaluated with the passive avoidance test (Figure 2); and finally, the drugs were tested also for their ethanol-potentiating action (Figure 3).

Table 2. BZR Ligand Affinity of New 8-Alkyloxy-/Aryloxy-/Arylpyrazolo[5,1-*c*][1,2,4]benzotriazine 5-Oxide 3-Substituted

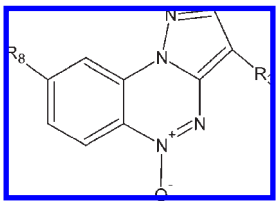

no.	R_3	R_8	I%[a] or K_i (nM)[b]
8	I	$O(CH_2)_7CH_3$	1616 ± 161
9	I	OC_6H_{11}	188 ± 18
10	I	OPh	8.6 ± 0.8
11	I	OCH_2Ph	1.1 ± 0.1
11R[c]	I	OCH_2Ph	1.0 ± 0.1
12	I	OCH_2-*o*-OMePh	0.42 ± 0.04
13	I	OCH_2-*p*-OMePh	4.5 ± 0.35
14	I	OCH_2-*o*-OCF_3Ph	6.6 ± 0.60
15	I	OCH_2-*p*-ClPh	11 ± 1.0
16(±)	I	$OCH(CH_3)Ph$	3.4 ± 0.26
16(+)	I	$OCH(CH_3)Ph$	605 ± 50.0
16(−)	I	$OCH(CH_3)Ph$	2.1 ± 0.10
17	I	OCH_2-4-Py	1.3 ± 0.10
18	I	OCH_2-2-thienyl	1.2 ± 0.10
19	I	OCH_2-2-furyl	0.8 ± 0.08
20	I	OCH_2CH_2Ph	43 ± 4.0
21(±)	I	$OCH(CH_3)CH_2Ph$	103 ± 10.0
22(±)	I	$OCH_2CH(CH_3)$ Ph	160 ± 15.0
23	I	O-2-naphthyl	94 ± 9.0
24	Cl	OPh	43 ± 4.0
25	3-thienyl	OPh	68 ± 6.5
26	$COOCH_2CH_3$	OPh	12 ± 1.1
27	$COOCH_2$-2-thienyl	OPh	0.7 ± 0.06
28	$COOCH_2$-*o*-OMePh	OPh	1.75 ± 0.15
29	H	OCH_2Ph	116 ± 11.1
30	$COOCH_2CH_3$	OCH_2Ph	2.1 ± 0.20
33	H	Ph	10%
36	$COOCH_2CH_3$	Ph	40%
37	I	Ph	966 ± 95
38	I	CH_2CH_2Ph	464 ± 45
39	I	CH=CH-Ph	2000 ± 200
41	Cl	Ph	45%
42	Br	Ph	802 ± 75

[a] Percent of inhibition of specific [^{3}H]Ro15-1788 binding at 10 μM concentration. [b] K_i value are means ± SEM of five determinations. [c] 5-Deoxide derivative.

Table 3. Additional Ligands Useful to Build the Pharmacophoric Model

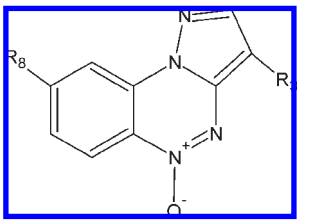

compd	R_3	R_8	K_i(nM)[a]	pharmacological in vivo activity
43[b]	$COOCH_2$-2-thienyl	Cl	6.8 ± 0.40	anxiolytic-like activity
44[c]	$COOCH_2$-2-thienyl	CH_3	1.41 ± 0.20	inactive
45[d]	$COOCH_2$-2-thienyl	CF_3	10 ± 1.0	
46[c]	$COOCH_2$-2-thienyl	OEt	0.85 ± 0.05	anxiogenic-like activity
47[b]	$COOCH_2$-*o*-OMePh	Cl	1.0 ± 0.10	anxiolytic-like activity
48[c]	$COOCH_2$-*o*-OMePh	CH_3	2.3 ± 0.20	inactive
49[d]	$COOCH_2$-*o*-OMePh	CF_3	5.8 ± 0.60	
50[c]	$COOCH_2$-*o*-OMePh	OEt	0.31 ± 0.03	anxiogenic-like activity

[a] K_i values are means ± SEM of five determinations. [b] See ref [24]. [c] See ref [25]. [d] Data not published.

7-chloro-1-methyl-5-phenyl-3*H*-1,4-benzodiazepin-2(1H)-one (diazepam) was used as reference molecule.

Effect on Motor Coordination. The effect of compounds **10**, **11**, **16**(+), **16**(−), and **17** was evaluated in comparison with diazepam in the mouse rota-rod test in order to evidence motor incoordination (Table 4, only the pretest and falls 30 min after treatment are reported). The reference compound (diazepam 1 mg/kg ip) increased the number of falls from the rotating rod, reaching statistical significance (Table 4). None of the newly synthesized substances induced any effect on the number of mouse falls from the rota-rod evaluated after 30 min; mice learned to stay on the rota-rod because the number of falls diminished in a time-dependent manner.

Effect against Chemically Induced Convulsions. Anticonvulsant activity was studied in mice using pentylenetetrazole (PTZ) as a chemical convulsant agent: the latency time (s) to shocks and convulsions was evaluated. Diazepam (1 mg/kg ip) completely protected against PTZ-induced shocks and convulsions (Table 4), while **10** (10 mg/kg po) and **11** (3 and 10 mg/kg po) reduced the convulsion latency. Compounds **10** (3 mg/kg po), **11** (30 mg/kg po), and **17** (3 and 10 mg/kg po) were devoid of any effect on PTZ-shock and convulsion latency. Compounds **16**(+) (10 mg/kg po) and **16**(−) (10 mg/kg po) increased in a significant manner the latency of both parameters, while at higher doses (30 mg/kg po) they did not modify shock and convulsion latency (Table 4).

Effects on Spontaneous Motility and Curiosity. One very common effect of the old benzodiazepine ligands is sedation. The hole-board test captures this kind of behavior as demonstrated by the significant reduction in spontaneous motility and curiosity exerted by diazepam at the dose of 3 mg/kg ip.

Experiments carried out on compounds **10**, **11**, **16**(+), **16**(−), and **17**, aimed to evaluate their effects on mouse spontaneous motility and explorative activity, revealed that compounds **10** (3 and 10 mg/kg po), **11** (3, 10, 30 mg/kg po), **16**(+) (10, 30, 50, 100 mg/kg po), **16**(−) (10, 30, and 100 mg/kg po) and **17** (3 and 10 mg/kg po) did not alter either spontaneous or explorative activity. By contrast, the dose of 50 mg/kg po **16**(−) was able to diminish curiosity and spontaneous motility (Table 5).

Effect on Anxiety. The effects on mouse anxiety of newly synthesized molecules, compared with diazepam, were studied using a light/dark box apparatus. Compounds **11** (3, 10, and 30 mg/kg po), **16**(−) (10 and 30 mg/kg po), and **16**(+) (10 and 30 mg/kg po) revealed good anxiolytic activity while **10**, at the doses of 1, 3, 10, and 30 mg/kg po, exhibited an anxiogenic effect. Compound **17** did not show any efficacy in this experimental model (Figure 1). The anxiolytic-like effects of **11** (10 and 30 mg/kg po), **16**(+) (30 mg/kg po), and **16**(−) (30 mg/kg po) and the anxiogenic effect of **10** (3 mg/kg po) were completely antagonized by flumazenil (dose of 100 mg/kg ip, a dose at which flumazenil was able to antagonize the anxiolytic effect of diazepam), suggesting that the agonist, inverse-agonist profile is at the Bzs site on the $GABA_A$ receptor of the newly synthesized ligands (Figure 1).

Effects on Learning and Memory. To clarify the effect that the newly synthesized compounds have on learning and memory processes, we investigated mouse performance in

Table 4. Motor Coordination and Anticonvulsant Effects of New Compounds in Comparison with Diazepam

treatment[a]		motor coordination rota-rod test (16 rpm) falls in 30 s			anticonvulsant activity		
compd	mg/kg po	n^b	pretest	30 min	n^b	shock latency (s)	convulsion latency (s)
CMC 1%[c]	0.1 mL	25	4.0 ± 0.5	1.3 ± 0.3	41(9)	253.1 ± 13.0	599.0 ± 37.6
diazepam	1 (ip)	6	4.8 ± 0.4	4.5 ± 0.4*[d]	15	no shocks***[f]	no convulsions***[f]
10	3	10	3.1 ± 0.6	0.9 ± 0.4	10(4)	264.7 ± 23.8	516.1 ± 113.8
	10	8	3.7 ± 0.8	0.6 ± 0.4	15(1)	243.6 ± 29.4	345.5 ± 74.5**[e]
11	3	10	4.6 ± 0.4	1.5 ± 0.3	12(0)	375.0 ± 15.0	380.2 ± 83.1*[d]
	10	10	4.6 ± 0.3	2.2 ± 0.6	15(4)	266.1 ± 32.1	360.8 ± 40.9**[e]
	30	10	4.5 ± 0.4	1.7 ± 0.4	15(5)	354.0 ± 59.6	479.7 ± 69.7
16(+)	10	14	4.7 ± 0.4	2.5 ± 0.3	27(6)	543.7 ± 63.1***[f]	733.5 ± 129.1***[f]
	30	14	4.8 ± 0.3	1.3 ± 0.2	29(8)	345.3 ± 19.5	607.7 ± 54.7
16(−)	10	16	3.9 ± 0.3	2.0 ± 0.4	25(6)	513.0 ± 51.1***[f]	1078.0 ± 150.5***[f]
	30	16	4.7 ± 0.3	1.6 ± 0.6	28(7)	323.7 ± 24.5	549.2 ± 47.0
17	3	10	3.3 ± 0.4	1.4 ± 0.4	8(2)	183.0 ± 16.8	565.8 ± 32.4
	10	10	3.2 ± 0.4	2.3 ± 0.6	8(2)	299.0 ± 46.6	610.9 ± 41.2

[a] Treatment with new compounds and diazepam (ip) was performed 30 min before the test. In the rota-rod test, treatment was performed 60 min before the test, and evaluation after 30 min. [b] Number of mice (number of dead mice). [c] Carboxymethylcellulose 1%. [d] $P < 0.05$. [e] $P < 0.01$. [f] $P < 0.001$ versus control mice.

Table 5. Effect of New Compounds on Animal Spontaneous Motility, in Comparison of Diazepam, in the Mouse Hole-Board Test

treatment[a]		hole-board		
compd	mg/kg po	n^b	hole	plane
CMC 1%	0.1 mL	31	33.5 ± 2.3	66.36 ± 1.6
diazepam	3 (ip)	11	13.4 ± 6.3**[d]	49.7 ± 6.6**[d]
10	3	10	38.0 ± 5.1	73.2 ± 6.2
	10	8	39.8 ± 2.9	63.8 ± 4.5
11	3	7	29.0 ± 7.0	54.3 ± 11.7
	10	9	22.7 ± 3.4	66.9 ± 9.1
	30	9	28.7 ± 4.7	54.5 ± 11.5
16(+)	10	10	25.1 ± 6.7	55.5 ± 14.2
	30	10	31.9 ± 2.2	59.7 ± 7.9
	50	10	39.3 ± 3.7	62.9 ± 3.4
	100	10	30.4 ± 3.4	80.0 ± 4.2
16(−)	10	10	27.0 ± 1.8	61.9 ± 6.8
	30	10	34.5 ± 3.2	56.8 ± 4.5
	50	10	13.3 ± 1.6***[e]	44.0 ± 3.2**[d]
	100	10	22.9 ± 1.3	59.2 ± 4.0
17	3	10	35.5 ± 1.5	93.9 ± 12.6
	10	10	36.9 ± 3.6	85.1 ± 9.6

[a] The test was performed 30 and 20 min after administration of compounds (po) and diazepam (ip) respectively. [b] Number of mice. [c] $P < 0.05$. [d] $P < 0.01$. [e] $P < 0.001$ versus control mice.

the passive avoidance test. In this assay, the parameters taken into consideration are training and retention latencies. While the training latencies did not differ in the various groups, some retention latencies were significantly different from the others. As shown in Figure 2, compounds **10** (1 and 3 mg/kg po), **11** (10 and 30 mg/kg po), and **17** (3 and 10 mg/kg po) improved mouse memory processes in a statistically significant manner. In contrast, compounds **16**(+) (10 and 30 mg/kg po) and **16**(−) (10 mg/kg po) decreased, in a statistically significant manner, the retention latency. In the same experimental test, flumazenil (100 mg/kg po) statistically significantly increased retention latency (Figure 2).

Effect on Ethanol-Induced Sleeping Time. In the ethanol-induced sleeping time test, compound **16**(+) at the doses of 10 and 30 mg/kg po, increased the duration of loss of righting reflex (Figure 3), while compounds **10** (3, 10 mg/kg po), **16**(−) (10, 30 mg/kg po), and **17** (3, 10 mg/kg po) did not modify it. On the contrary, **11**, but only at the dose of 30 mg/kg po, reduced the same parameter in a statistically significant manner, while at the other doses (3, 10 mg/kg po) it did not modify this parameter. As expected, the reference drug, diazepam (Diaz., ip), enhanced sedation in a statistically significant manner.

Pharmacophoric Map. The pharmacophoric map was drawn using all new synthesized molecules (Table 2) and other ligands previously reported (compounds **43**−**50**,[24,25] Table 3).

Pharmacophoric point (Pp) identification, search for common points, and the conformation alignment are outlined in the experimental section.

We found four common "pharmacophoric points" out of all studied molecules: a lipophilic point (Lp-1) and three hydrogen bond interaction points (HBp-1a, HBp-1b, and HBp-2). The two possible positions, HBp-1a and HBp-1b, define the same hydrogen interaction area, labeled HBp-1a,b, in our opinion. The similarity in "pharmacophoric points" positions among all molecules, calculated from the average difference in intramolecular distances among the four points (distance difference sum square, see Experimental Section), is sufficiently high (the average is less than 1 Å). We can reasonably expect that the presence of these four features is necessary for binding recognition, but it is not sufficient to explain the difference in receptor binding affinity of all the studied molecules. In fact, binding data indicate that molecules endowed with the best receptor affinity have an acceptor hydrogen bond atom (oxygen) at position 8 and a lipophilic group at position 3. Other pharmacophoric points have to be considered, and the pharmacophore map shows a further hydrogen bond interaction area (HBp-3) near Lp-1 and a new lipophilic area, Lp-2. From the pharmacophoric model, four structural typologies of ligands can be achieved, depending on the type of atom or group (hydrogen bond acceptor, or not) in position 3 or 8: in *typology 1*, no acceptor in either position; in *typology 2*,

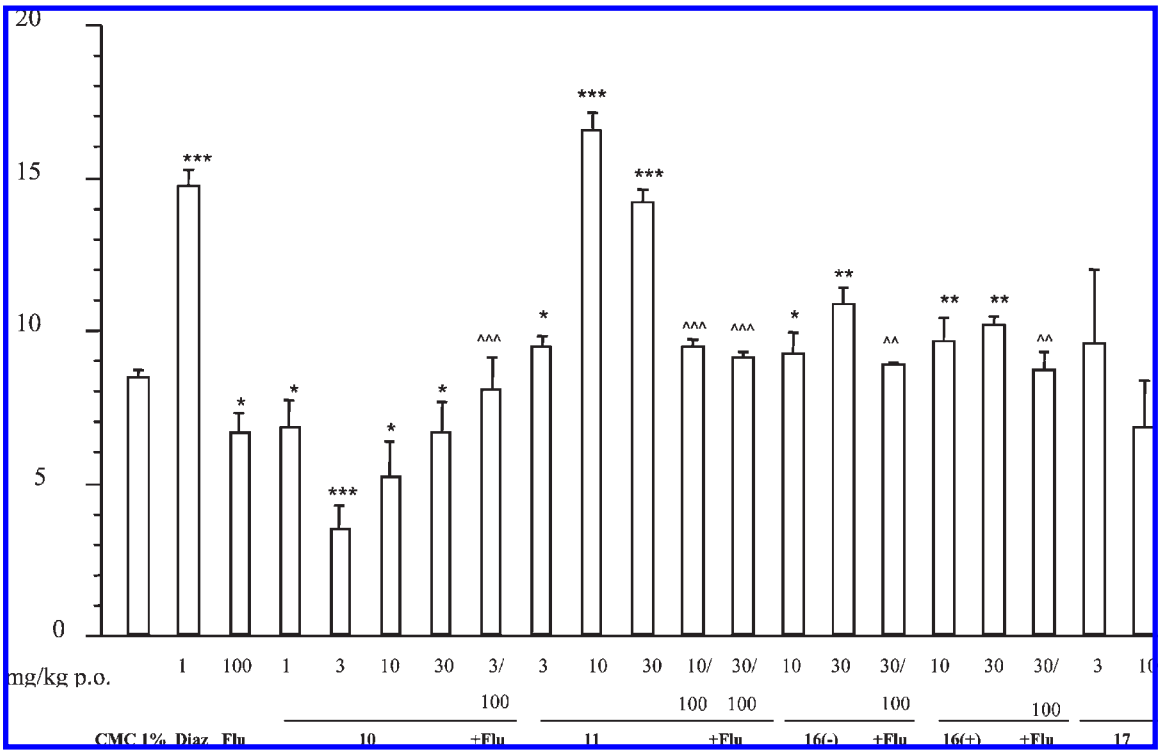

Figure 1. Antianxiety activity. Effect of compounds **10**, **11**, **16**(−), **16**(+), and **17** in comparison with diazepam (Diaz., ip) on mouse light−dark box test. Each column represents the time, expressed in s, spent in illuminated compartment. Treatment with compounds (po) and flumazenil (Flu., ip) was performed 30 min and with diazepam (Diaz., ip) 20 min before the test. Each column represents the mean ± SEM of 15−20 mice. $^{*}P < 0.05$, $^{**}P < 0.01$, $^{***}P < 0.001$ versus controls. $^{\wedge\wedge}P < 0.01$, $^{\wedge\wedge\wedge}P < 0.001$ versus **10**-treated, **11**-treated, or **16**(−)-treated mice.

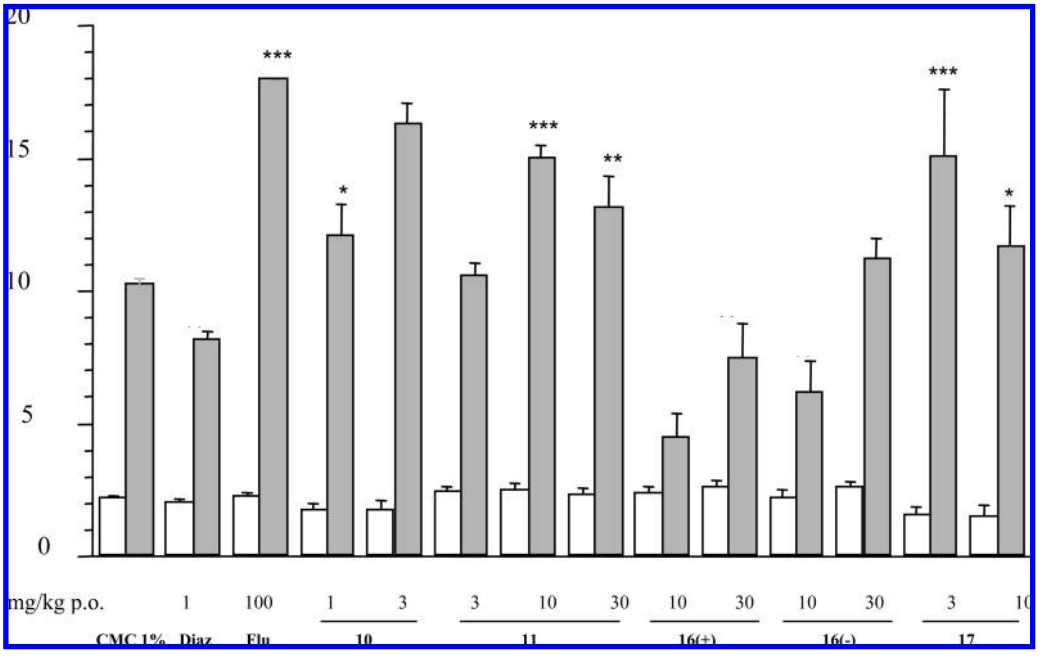

Figure 2. Learning and memory performance. Effect of compounds **10**, **11**, **16**(+), **16**(−), and **17** in comparison with diazepam (Diaz., ip) and flumazenil (Flu., ip) on mouse passive avoidance test. White histograms represent the training latency and gray histograms represent the retention latency. Mice were treated 30 min before the training test. The retention test was performed 24 h later. Each column represents the mean ± SEM of 15−20 mice. $^{*}P < 0.05$, $^{**}P < 0.01$, $^{***}P < 0.001$ versus controls.

acceptor in both positions; in *typology 3*, no acceptor in position 3 and acceptor in position 8; in *typology 4*, acceptor in position 3 and no acceptor in position 8.

Molecules belonging to structural *typology 1* (compounds **33**, **37**−**39**, **41**−**42**) showed no or negligible receptor binding affinity (Table 2) because they cannot provide efficient anchorage with a hydrogen bond because of lack of an acceptor group.Molecules having hydrogen bond acceptors at positions 3 and 8 (i.e., structural *typology 2*) are endowed with high binding affinity (compounds

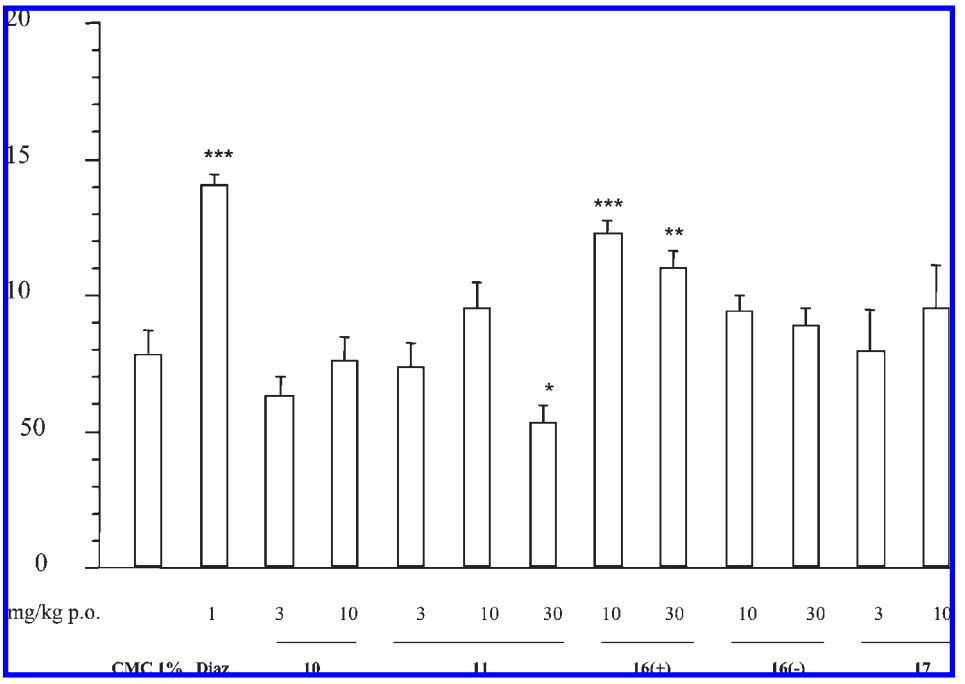

Figure 3. Ethanol-induced sleeping time effect. Effect of compounds **10**, **11**, **16**(+), **16**(−), and **17** in comparison with diazepam (Diaz., ip) on mouse ethanol-induced sleeping time. Each column represents the mean ± SEM of 15−22 mice. Substances were administered 30 min after ethanol (4 g/kg ip). $*P < 0.05$, $**P < 0.01$, $***P < 0.001$ versus controls.

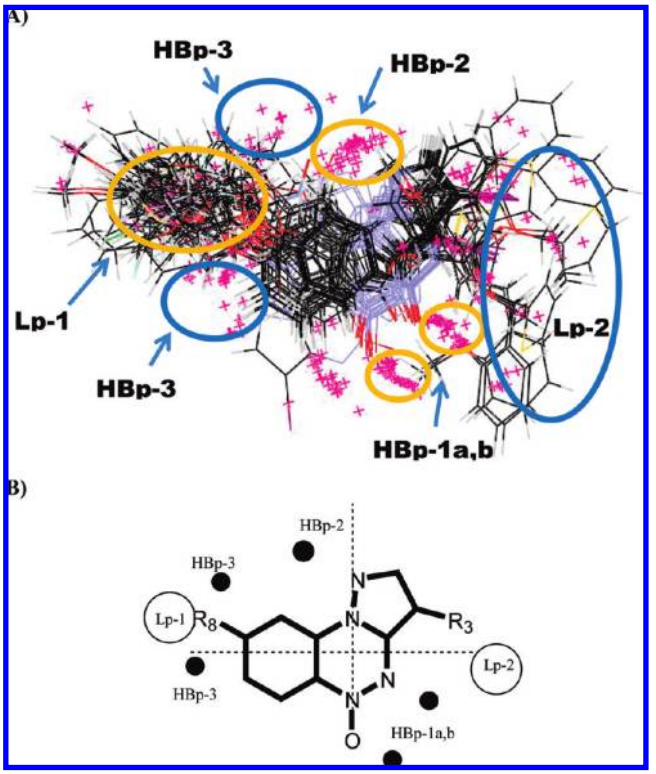

Figure 4. (A) Overlapping of ligand conformations considered in this study (all newly synthesized and some previously reported, see text). In the figure are reported the essential interaction points for binding recognition (HBp-1a,b, HBp-2, and Lp-1, yellow circles) and the important areas for affinity modulation (HBp-3 and Lp-2, blue circles). (B) Schematic representation of pharmacophoric map.

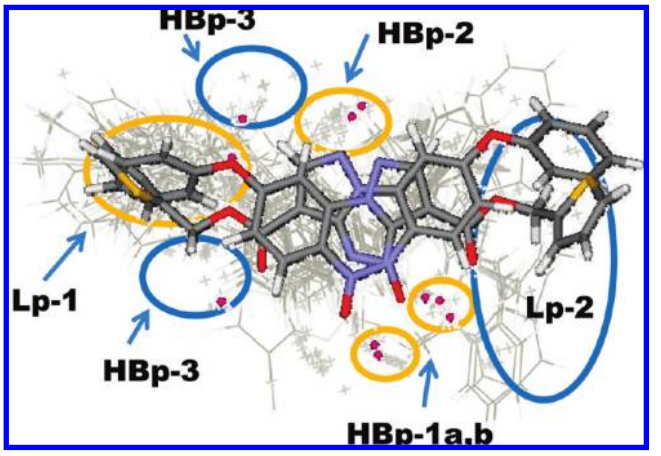

Figure 5. Compound **27**, structure *typology 2*, is evidenced in the pharmacophoric model. It presents two possible orientations in the model and in both of them the pharmacophoric points (red points) fall in the right hydrogen bond areas.

26, **27**, **28**, **29**) because they can easily orient themselves in two modes (by a 180° rotation on vertical axis) into the pharmacophore model. Figure 5 presents the two conformations of compound **27**. In both orientations, the pharmacophoric groups are correctly set to form efficient hydrogen bonds.

Molecules having a hydrogen bond acceptor only at position 8 (i.e., structural *typology 3*) are endowed with good (**10**−**20**) or moderate binding affinity (**8**, **9**, **21**, **22**). For these latter compounds, probably the 8-substituent is too bulky. All molecules present only one orientation with the hydrogen bond acceptor always in the HBp-3 area. Three conformations of compound **12** are depicted in Figure 6.

Molecules having a hydrogen bond acceptor only at position 3 (compounds **36**, **48**), belonging to structural *typology 4*, present two different orientations as depicted in Figure 7A. In the first orientation, the 3-substituent (hydrogen bond acceptor) can engage a hydrogen bond in the HBp-3 area; in the

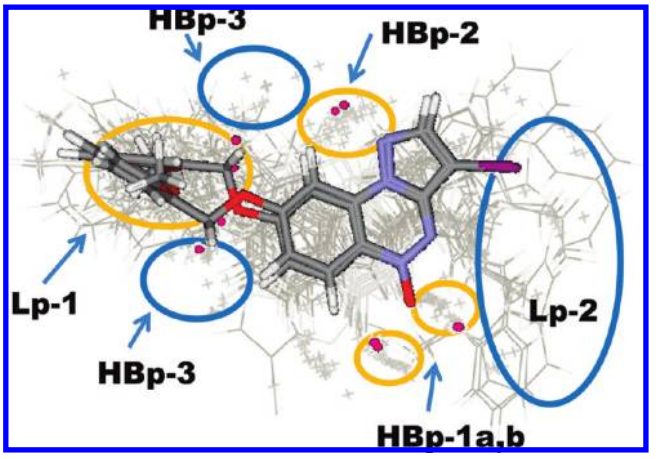

Figure 6. Compound **12**, structure *typology 3*, is evidenced in the pharmacophoric model. It presents only one possible orientation in the model with the hydrogen bond acceptor always in the HBp-3 area. The pharmacophoric points (red points) fall in the right hydrogen bond areas.

second, by means of the double 180° rotation on the horizontal and vertical axis, the oxygen of *N*-oxide group and N1-pyrazole could engage a hydrogen bond in the same HBp-3 area and the 3-substituent interacts with lipophilic area Lp-2. To explain the different binding affinity of **36** and **48** (I% 40 vs K_i = 2.3 nM), we can hypothesize that in the two possible orientations the 8-phenyl ring of compound **36** interacts with a probable steric repulsive area near Lp-2 or Lp-1 (Figure 7B). The presence of the steric hindrance near Lp-1 has already been hypothesized in the discussion of *typology 3* molecules, which present a bulky substituent.

The probable positions of HBp-3 are those reported in Figure 4, although this cannot be distinctly determined because of the free rotation of the acceptor substituent in *typology 3* and because of the two different orientations (180° rotation on vertical axis) in typologies 2 and 4.

To compare our pharmacophoric model with Cook's "unified pharmacophore/receptor model",[33] two ligands (CGS 9698 and diazepam), already used by Cook, were inserted in our map. These ligands, in their different orientations, form an efficient interaction with the areas of our model (Figures 8 and 9). In comparison with Cook's model,[33] we found that lipophilic and steric interaction areas correspond, as well as the hydrogen bond interaction areas. Lipophilic points Lp-1 and Lp-2 and hydrogen bond interaction points HBp-1 and HBp-2 coincide, respectively, with the L_{Di}, L-1/L-2, H1 and H2 sites of the Cook model.[33] Instead, the HBp-3 (corresponding to the acceptor hydrogen bond site A2 in Cook's model) probably is an acceptor/donor hydrogen bond area, which is not essential for receptor recognition but modulates the affinity of ligands. This hypothesis is verified by observing the CGS 9896 interaction within our pharmacophoric model, particularly the interaction of quinoline NH in the HBp-3.

In both orientations, diazepam has hydrogen bond interactions with HBp-1a,b and HBp-2 and not with HBp-3, and lipophilic interactions with Lp-1 and Lp-2.

Conclusion

All new compounds (**8**−**30**, **11R**, **33**, **36**−**39**, **41**, and **42**) were studied in in vitro tests and **10**, **11**, **16**(+), **16**(−), and **17** were evaluated in in vivo experiments, as well. The pharmacophoric

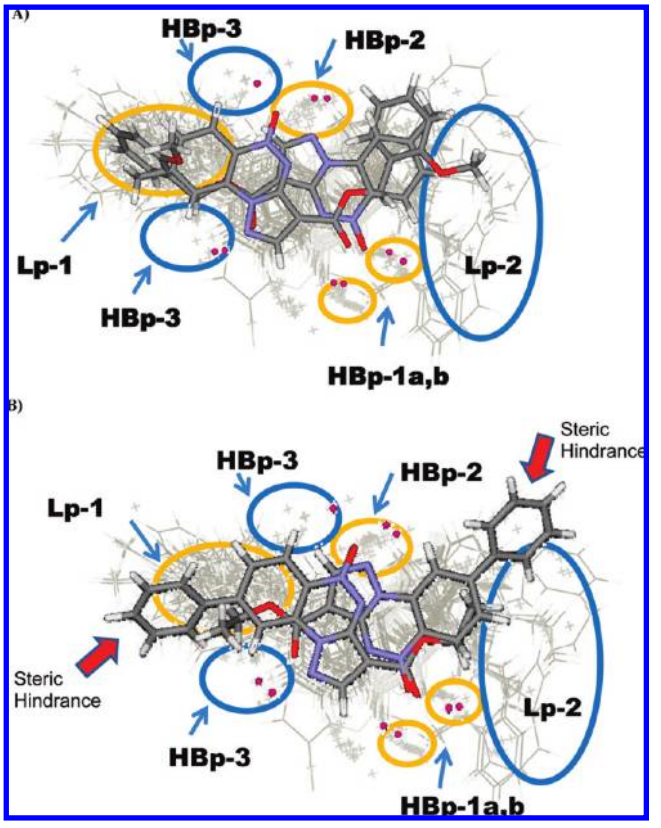

Figure 7. (A) Compound **48**,[25] structure *typology 4* that fits in the pharmacophoric model in the two possible orientations. (B) It justified the inactivity of compound **36** despite the two possible orientation that it can assume. The areas with steric hindrance are evidenced with red arrows and are due to the phenyl ring at the position 8.

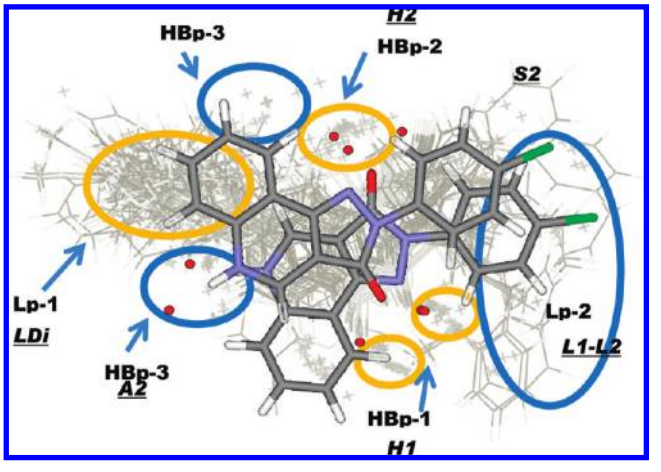

Figure 8. CGS9896 in our pharmacophoric model. The H1, H2, L1-L2, A2, and L_{Di} represent the anchor points of the Cook model.

model was set up using all new synthesized molecules (Table 2) and other ligands previously reported (compounds **43**−**50**,[24,25] Table 3). This obtained model was compared with a frequently used BzR pharmacophore (Cook et al.[34]), and some of the similarities and differences in these models may be seen.

From these findings, it emerges that: (a) the hydrogen bond point HBp-3 (Figure 4) is endowed with different features compared to A2 (A2 represents a hydrogen bond acceptor site in the Cook model[34]). From the literature data[35] we know that

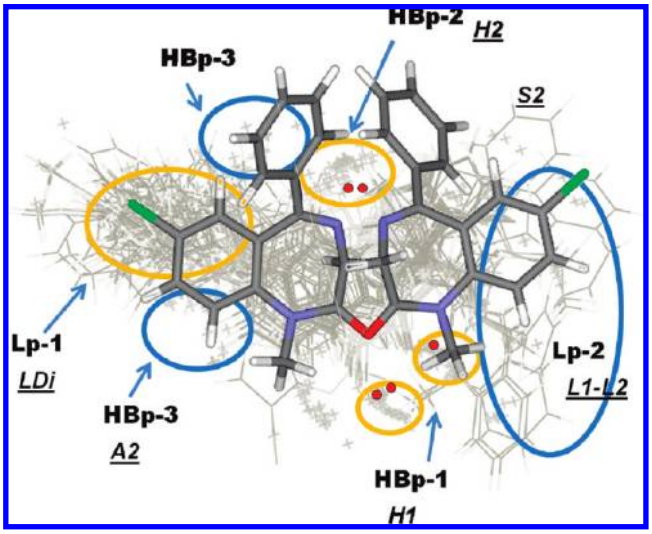

Figure 9. Diazepam in our pharmacophoric model. The H1, H2, L1-L2, A2, and L_{Di} represent the anchor points of the Cook model.

the descriptor A2 represents a necessary area for potent inverse agonist activity in vivo. The fact that our ligands (**10**, **11**, and **17**) have anxiogenic and/or pro-mnemonic activity (inverse agonist activity) strengthens the hypothesis of the bifunctional features, acceptor/donor, of the HBp-3 area. (b) Biological data confirm that the presence at position 8 of the pyrazolobenzotriazine core of a $\pi-\pi$ system, represented by an aryloxy-, aryl-/heteroarylalkyloxy group, confers high binding affinity, as ligands **11**, **12**, **17**, **18**, and **19** (K_i range: $0.42 < \text{nM} < 1.3$) show. (c) Examination of the pharmacological results leads us to define a behavioral profile for all tested compounds (**10**, **11**, **16**(+), **16**(−), and **17**). In particular, enantiomers **16**(+) and **16**(−), which greatly vary in terms of binding affinity (**16**(+) $K_i = 3.4$ nM **16**(−) $K_i = 605$ nM), have a similar pharmacological profile (anxiolytic-like activity) at the same doses (10, 30 mg/kg). Because this deviation between the in vitro and in vivo data cannot be explained only by evoking metabolic transformations (stability, inversion of configuration) or other factors (e.g., differences in receptor efficacy), an in-depth study will be undertaken to understand their in vivo behavior. Compound **17** (8-pyridin-4-ylmethoxy derivative) endowed with very good affinity ($K_i = 1.3$ nM), stands out because of its ability to selectively improve mice memory performance without anxiolytic-like and side effects. Compound **11** (8-benzyloxy derivative), an isoster of **17** with a similar affinity value ($K_i = 1.1$ nM), shows anxiolytic-like and pro-mnemonic properties, while compound **10** (8-phenoxy derivative, $K_i = 8.6$ nM) shows anxiogenic and pro-mnemonic activity. These well-defined pharmacological profiles are mediated by acting on the benzodiazepine site on $GABA_A$ receptor because are all antagonized by flumazenil.

To date, numerous investigations have proposed that the pharmacological effects of ligands at the benzodiazepine site on $GABA_A$ receptor are mediated via different subtypes (α_1-, α_2-, α_3-, and α_5-containing $GABA_A$ receptors).

However, to hypothesize a correlation between the pharmacological profile of our compounds and selective affinity and/or selective efficacy, without confirmation from thorough biological tests, would be hazardous. Because it has been shown that the α_2- and the α_3-subtypes are involved in anxiety disorder and the α_5-subtype plays a role in cognitive processes,[1,6−17] further studies are necessary to demonstrate this probable correlation. Small modifications in the lipophilic/hydrophilic balance may be responsible for the different pharmacological activity of compounds **11** and **17**, which would permit us to design selective anxiolytic and pro-mnemonic agents.

Experimental Section

Chemistry. Melting points were determined with a Gallenkamp apparatus and were uncorrected. Silica gel plates (Merk F_{254}) and silica gel 60 (Merk 70−230 mesh) were used for analytical and column chromatography, respectively. The structures of all compounds were supported by their IR spectra (KBr pellets in nujol mulls, Perkin-Elmer 1420 spectrophotometer) and ^{1}H NMR data (measured with a Bruker 400 MHz). Chemical shifts were expressed in δ ppm, using DMSO-d_6 or $CDCl_3$ as solvent. The coupling constant values ($J_{H6-H7,\ H7-H6}$; $J_{H7-H9,\ H9-H7}$) were in agreement with the assigned structure. The chemical and physical data of new compounds are shown in Table 1. All new compounds possess a purity ≥95%: microanalyses were performed with a Perkin-Elmer 260 analyzer for C, H, N. Optical rotation was measured at a concentration of 1 g/100 mL ($c = 1$, $CHCl_3$), unless otherwise stated, with a Perkin-Elmer polarimeter (accuracy ±0.002°).

General Procedure for the Synthesis of 8−30. Starting from compounds **1**−**7** (see Scheme 1), the final products **24**−**30** were obtained. The reaction was carried out in 10 mL of dichloromethane to which was added the starting material (0.3 mmol), 5 mL of 40% sodium hydroxide solution, 0.1 mol of tetrabutylammonium bromide, and the suitable alcohol in large excess (5 mL) under vigorous stirring (temperature and time specified for each compound). The reaction was monitored by TLC, and when the starting material disappeared, the organic layer was separated and the aqueous layer extracted twice with 10 mL of dichloromethane. The combined organic extracts were evaporated and the residue was recovered with isopropyl ether and recrystallized by suitable solvent.

3-Iodio-8-octyloxypyrazolo[5,1-*c*][1,2,4]benzotriazine 5-Oxide (8). From **1**, 3-iodo-8-chloropyrazolo[5,1-*c*][1,2,4]benzotriazine 5-oxide,[28,26] and octanol, at 70 °C for 3 h. Yellow crystals. TLC eluent: *i*-propyl ether/cyclohexane 8:3 v/v. ^{1}H NMR ($CDCl_3$) δ 8.46 (d, 1H, H-6), 8.10 (s, 1H, H-2), 7.67 (d, 1H, H-9), 7.16 (dd, 1H, H-7), 4.22 (t, 2H, OCH_2), 1.90 (m, 2H, CH_2), 1.50 (m, 2H, CH_2), 1.32 (m, 8H, CH_2), 0.90 (t, 3H, CH_3). Anal. C, H, N.

3-Iodio-8-cyclohexyloxypyrazolo[5,1-*c*][1,2,4]benzotriazine 5-Oxide (9). From **1**,[26,28] and cyclohexanol, at 40 °C for 8 h. Yellow crystals. TLC eluent: chloroform, ^{1}H NMR ($CDCl_3$) δ 8.45 (d, 1H, H-6), 8.09 (s, 1H, H-2), 7.65 (d, 1H, H-9), 7.13 (dd, 1H, H-7), 4.59 (m, 1H, CH−O), 2.07 (m, 2H, cyclohexane), 1.86 (m, 2H, cyclohexane), 1.65 (m, 3H, cyclohexane), 1.48 (m, 3H, cyclohexane). Anal. C, H, N.

3-Iodio-8-phenoxypyrazolo[5,1-*c*][1,2,4]benzotriazine 5-Oxide (10). From **1**,[26,28] and phenol, at 40 °C for 8 h. Yellow crystals. TLC eluent: chloroform. ^{1}H NMR ($CDCl_3$) δ 8.52 (d, 1H, H-6), 8.05 (s, 1H, H-2), 7.68 (d, 1H, H-9), 7.52 (t, 2H, H-3′ and H-5′ Ph), 7.37 (t, 1H, H-4′ Ph), 7.26 (dd, 1H, H-7), 7.19 (dd, 2H, H-2′ and H-6′ Ph). Anal. C, H, N.

3-Iodio-8-benzyloxypyrazolo[5,1-*c*][1,2,4]benzotriazine 5-Oxide (11). From **1**,[26,28] and benzyl alcohol, at room temperature for 12 h. Yellow crystals. TLC eluent: chloroform. ^{1}H NMR ($CDCl_3$) δ 8.48 (d, 1H, H-6), 8.10 (s, 1H, H-2), 7.79 (d, 1H, H-9), 7.48 (m, 5H, Ph), 7.24 (dd, 1H, H-7), 5.32 (s, 2H, CH_2O). Anal. C, H, N.

3-Iodio-8-(*o*-methoxybenzyloxy)pyrazolo[5,1-*c*][1,2,4]benzotriazine 5-Oxide (12). From **1**,[26,28] and *o*-methoxybenzyl alcohol, at 50 °C for 2 h. Yellow crystals. TLC eluent: chloroform. ^{1}H NMR ($CDCl_3$) δ 8.47 (d, 1H, H-6), 8.11 (s, 1H, H-2), 7.87 (d, 1H, H-9), 7.48 (d, 1H, H-6′ Ph), 7.38 (t, 1H, H-4′ Ph), 7.24 (dd, 1H, H-7), 7.03 (t, 1H, H-5′ Ph), 6.98 (d, 1H, H-3′ Ph), 5.37 (s, 2H, CH_2O), 3.95 (s, 3H, OCH_3). Anal. C, H, N.

3-Iodio-8-(*p*-methoxybenzyloxy)pyrazolo[5,1-*c*][1,2,4]benzotriazine 5-Oxide (13). From **1**,[26,28] and *p*-methoxybenzyl alcohol, at

70 °C for 2 h. Yellow crystals. TLC eluent: *i*-propyl ether/cyclohexane 8:3 v/v. ^{1}H NMR ($CDCl_3$) δ 8.48 (d, 1H, H-6), 8.11 (s, 1H, H-2), 7.79 (d, 1H, H-9), 7.43 (d, 2H, H-2′ and H-6′ Ph), 7.21 (dd, 1H, H-7), 6.98 (d, 2H, H-3′ and H-5′ Ph), 5.24 (s, 2H, CH_2O), 3.85 (s, 3H, OCH_3). Anal. C, H, N.

3-Iodio-8-(*o*-trifluoromethoxybenzyloxy)pyrazolo[5,1-*c*][1,2,4]-benzotriazine 5-Oxide (14). From **1**,[26,28] and *o*-trifluoromethoxybenzyl alcohol, at 70 °C for 2 h. Yellow crystals. TLC eluent: toluene/ethyl acetate/acetic acid 8:2:1 v/v/v, ^{1}H NMR (DMSO-d_6) δ 8.39 (m, 2H, H-2 and H-6), 7.81 (d, 1H, H-9), 7.75 (d, 1H, H-3′ Ph), 7.57 (dd, 1H, H-6′ Ph), 7.48 (m, 2H, H-4′ and H-5′ Ph), 7.35 (dd, 1H, H-7), 5.50 (s, 2H, CH_2O). Anal. C, H, N.

3-Iodio-8-(*p*-chlorobenzyloxy)pyrazolo[5,1-*c*][1,2,4]benzotriazine 5-Oxide (15). From **1**,[26,28] and *p*-chlorobenzyl alcohol, at 40 °C for 2.30 h. Yellow crystals. TLC eluent: chloroform. ^{1}H NMR ($CDCl_3$) δ 8.49 (d, 1H, H-6), 8.11 (s, 1H, H-2), 7.77 (d, 1H, H-9), 7.44 (s, 4H, Ph), 7.23 (dd, 1H, H-7), 5.29 (s, 2H, CH_2O). Anal. C, H, N.

3-Iodo-8-(1-phenylethoxy)pyrazolo[5,1-*c*][1,2,4]benzotriazine 5-Oxide (16(±)). From **1**,[26,28] and (±)1-phenylethanol, at 50 °C for 12 h. Yellow crystals. TLC eluent: toluene/ethyl acetate/acetic acid 8:2:1 v/v/v. ^{1}H NMR ($CDCl_3$) δ 8.41 (d, 1H, H-6), 8.04 (s, 1H, H-2), 7.62 (d, 1H, H-9), 7.42 (m, 4H, Ph), 7.32 (m, 1H, Ph), 7.17 (dd, 1H, H-7), 5.60 (q, 1H, CH), 1.78 (d, 3H, CH_3). Anal. C, H, N.

3-Iodo-8-(1-phenylethoxy)pyrazolo[5,1-*c*][1,2,4]benzotriazine 5-Oxide (16(+)). From **1**,[26,28] and (*R*)(+)1-phenylethanol, at 50 °C for 12 h. Yellow crystals. TLC eluent: *i*-propyl ether/cyclohexane 8:3 v/v. ^{1}H NMR ($CDCl_3$) δ 8.41 (d, 1H, H-6), 8.05 (s, 1H, H-2), 7.63 (d, 1H, H-9), 7.38 (m, 5H, Ph), 7.16 (dd, 1H, H-7), 5.60 (q, 1H, CH), 1.77 (d, 3H, CH_3). $[\alpha]^{20°}_D$ = +220. Anal. C, H, N.

3-Iodo-8-(1-phenylethoxy)pyrazolo[5,1-*c*][1,2,4]benzotriazine 5-Oxide (16(−)). From **1**,[26,28] and (*S*)(−)1-phenylethanol, at 50 °C for 12 h. Yellow crystals. TLC eluent: *i*-propyl ether/cyclohexane 8:3 v/v. ^{1}H NMR ($CDCl_3$) δ 8.41 (d, 1H, H-6), 8.05 (s, 1H, H-2), 7.63 (d, 1H, H-9), 7.38 (m, 5H, Ph), 7.16 (dd, 1H, H-7), 5.59 (q, 1H, CH), 1.78 (d, 3H, CH_3). $[\alpha]^{20°}_D$ = −220. Anal. C, H, N.

3-Iodo-8-(pyridin-4-ylmethoxy)pyrazolo[5,1-*c*][1,2,4]benzotriazine 5-Oxide (17). From **1**,[26,28] and pyridine-4-methanol, at 70 °C for 25 min. The reaction rapidly changes color in function of temperature: from yellow to brown and then green at hot temperature. Yellow gold crystals. TLC eluent: chloroform/methanol 10:1 v/v. ^{1}H NMR ($CDCl_3$) δ 8.70 (d, 2H, H-2′ and H-6′ Py), 8.52 (d, 1H, H-6), 8.10 (s, 1H, H-2), 7.78 (d, 1H, H-9), 7.44 (d, 2H, H-3′ and H-5′ Py), 7.28 (dd, 1H, H-7), 5.35 (s, 2H, CH_2O). Anal. C, H, N.

3-Iodo-8-(thien-2-ylmethoxy)pyrazolo[5,1-*c*][1,2,4]benzotriazine 5-Oxide (18). From **1**,[26,28] and thiophen-2-methanol, at 70 °C for 3 h. Yellow crystals. TLC eluent: toluene/ethyl acetate/acetic acid 8:2:1 v/v/v. ^{1}H NMR ($CDCl_3$) δ 8.50 (d, 1H, H-6), 8.11 (s, 1H, H-2), 7.82 (d, 1H, H-9), 7.42 (dd, 1H, H-3′ thiophene), 7.25 (m, 2H, H-7 and H-5′ thiophene), 7.08 (m, 1H, H-4′ thiophene), 5.50 (s, 2H, CH_2O). Anal. C, H, N.

3-Iodo-8-(fur-2-ylmethoxy)pyrazolo[5,1-*c*][1,2,4]benzotriazine 5-Oxide (19). From 3-iodo-8-chloropyrazolo[5,1-*c*][1,2,4]benzotriazine 5-oxide[26,28] and furan-2-methanol (furfuryl alcohol), at 70 °C for 3 h. Yellow crystals. TLC eluent: toluene/ethyl acetate/acetic acid 8:2:1 v/v/v. ^{1}H NMR ($CDCl_3$) δ 8.50 (d, 1H, H-6), 8.12 (s, 1H, H-2), 7.85 (d, 1H, H-9), 7.52 (dd, 1H, H-3′ furane), 7.20 (dd, 1H, H-7), 6.60 (dd, 1H H-5′ furane), 6.43 (m, 1H, H-4′ furane), 5.25 (s, 2H, CH_2O). Anal. C, H, N.

3-Iodo-8-(2-phenylethoxy)pyrazolo[5,1-*c*][1,2,4]benzotriazine 5-Oxide (20). From **1**[26,28] and 2-phenylethanol, at 40 °C for 8 h. Yellow crystals. TLC eluent: chloroform. ^{1}H NMR ($CDCl_3$) δ 8.44 (d, 1H, H-6), 8.08 (s, 1H, H-2), 7.65 (d, 1H, H-9), 7.35 (m, 5H, Ph), 7.15 (dd, 1H, H-7), 4.43 (t, 2H, CH_2O), 3.23 (t, 2H, CH_2). Anal. C, H, N.

3-Iodo-8-(1-methyl-2-phenylethoxy)pyrazolo[5,1-*c*][1,2,4]benzotriazine 5-Oxide (21(±)). From **1**[26,28] and 1-phenylpropan-2-ol, at 70 °C for 3 h. Yellow crystals. TLC eluent: toluene/ethyl acetate/acetic acid 8:2:1 v/v/v. ^{1}H NMR ($CDCl_3$) δ 8.34 (d, 1H, H-6), 8.00 (s, 1H, H-2), 7.55 (d, 1H, H-9), 7.23 (m, 5H, Ph), 7.01 (dd, 1H, H-7), 4.82 (m, 1H, CH), 3.09 (dd, 1H, CH_2), 2.90 (dd, 1H, CH_2), 1.38 (d, 3H, CH_3). Anal. C, H, N.

3-Iodo-8-(2-methyl-2-phenylethoxy)pyrazolo[5,1-*c*][1,2,4]benzotriazine 5-Oxide, 22(±). From **1**[26,28] and 2-phenylpropan-1-ol, at 70 °C for 3 h. Yellow crystals. TLC eluent: toluene/ethyl acetate/acetic acid 8:2:1 v/v/v. ^{1}H NMR ($CDCl_3$) δ 8.35 (d, 1H, H-6), 8.00 (s, 1H, H-2), 7.55 (d, 1H, H-9), 7.25 (m, 5H, Ph), 7.05 (dd, 1H, H-7), 4.22 (dd, 1H, CH_2O), 4.15 (dd, 1H, CH_2O), 3.28 (m, 1H, CH), 1.40 (d, 3H, CH_3). Anal. C, H, N.

3-Iodo-8-(2-naphthyloxy)pyrazolo[5,1-*c*][1,2,4]benzotriazine 5-Oxide (23). From **1**,[26,28] and 2-phenylethanol, at 70 °C for 12 h. Yellow crystals. TLC eluent: chloroform; ^{1}H NMR (DMSO-d_6) δ 8.47 (d, 1H, H-6), 8.26 (s, 1H, H-2), 8.15 (d, 1H, H-4′ napht.), 8.05 (d, 1H, H-8′ napht.), 7.97 (d, 1H, H-5′ napht.), 7.85 (d, 1H, H-9), 7.60 (m, 2H, H-7′ and H8′ napht.), 7.51 (d, 1H, H-1 napht.), 7.46 (dd, 1H, h-3′ napht.), 7.42 (dd, 1H, H-7). Anal. C, H, N.

3-Chloro-8-phenoxypyrazolo[5,1-*c*][1,2,4]benzotriazine 5-Oxide (24). From **2**[26] and phenol, at 40 °C for 8 h. Yellow crystals. TLC eluent: chloroform. ^{1}H NMR ($CDCl_3$) δ 8.50 (d, 1H, H-6), 8.00 (s, 1H, H-2), 7.68 (d, 1H, H-9), 7.50 (t, 2H, H-3′ and H-5′ Ph), 7.35 (t, 1H, H-4′ Ph), 7.23 (dd, 1H, H-7), 7.20 (dd, 2H, H-2′ and H-6′ Ph). Anal. C, H, N.

3-(Thien-3-yl)-8-phenoxypyrazolo[5,1-*c*][1,2,4]benzotriazine 5-oxide (25). From **3**[23] and phenol, at 60 °C for 12 h. Yellow crystals. TLC eluent: toluene/ethyl acetate 8:3 v/v. ^{1}H NMR ($CDCl_3$) δ 8.55 (d, 1H, H-6), 8.26 (s, 1H, H-2), 7.90 (d, 1H, H-2′ thiophene), 7.70 (d, 1H, H-9), 7.66 (dd, 1H, H-4′ thiophene), 7.52 (m, 2H, H-3′ and H-5′ Ph), 7.44 (m, 1H, H-5′ thiophene), 7.36 (m, 1H, H-4′ Ph), 7.25 (dd, 1H, H-7), 7.21 (m, 2H, H-2′ and H-6′ Ph). Anal. C, H, N.

3-Ethoxycarbonyl-8-phenoxypyrazolo[5,1-*c*][1,2,4]benzotriazine 5-oxide (26). From **4**[29] and phenol, at 40 °C for 8 h. Yellow crystals. TLC eluent: toluene/ethyl acetate 8:3 v/v. ^{1}H NMR ($CDCl_3$) δ 8.55 (d, 1H, H-6), 8.47 (s, 1H, H-2), 7.71 (d, 1H, H-9),; 7.54 (t, 2H, H-3′ and H-5′ Ph), 7.38 (t, 1H, H-4′ Ph), 7.33 (dd, 1H, H-7), 7.20 (dd, 2H, H-2′ and H-6′ Ph), 4.40 (q, 2H, CH_2), 1.40 (t, 3H, CH_3). Anal. C, H, N.

3-(2-Thienylmethoxycarbonylmethyl)-8-phenoxypyrazolo[5,1-*c*][1,2,4]benzotriazine 5-Oxide (27). From **5**[24] and phenol, at 30 °C for 2 h. Yellow crystals. TLC eluent: toluene/ethyl acetate/acetic acid 8:2:1 v/v/v. ^{1}H NMR ($CDCl_3$) δ 8.55 (d, 1H, H-6), 8.47 (s, 1H, H-2), 7.71 (d, 1H, H-9), 7.53 (t, 2H, H-3′ and H-5′ Ph), 7.35 (m, 3H, H-4′ Ph, H-5″ thiophene and H-7), 7.25 (dd, 1H, H-3″ thiophene), 7.20 (d, 2H, H-2′ and H-6′ Ph), 7.03 (dd, 1H, H-4″ thiophene), 5.52 (s, 2H, CH_2). Anal. C, H, N.

3-(2-Methoxyphenoxycarbonylmethyl)-8-phenoxypyrazolo[5,1-*c*][1,2,4]benzotriazine 5-Oxide (28). From **6**[24] and phenol, at 30 °C for 2 h. Yellow crystals. TLC eluent: toluene/ethyl acetate/acetic acid 8:2:1 v/v/v. ^{1}H NMR ($CDCl_3$) δ 8.54 (d, 1H, H-6), 8.49 (s, 1H, H-2), 7.71 (d, 1H, H-9), 7.58 (d, 1H, H-6″ Ph), 7.52 (t, 2H, H-3′ and H-5′ OPh), 7.38 (t, 1H, H-4′ OPh), 7.32 (m, 2H, H-7 and H-4″ Ph), 7.20 (d, 2H, H-2′ and H-6′ OPh), 7.01 (t, 1H, H-5″ Ph), 6.91 (d, 1H, H-3″ Ph), 5.50 (s, 2H, CH_2), 3.90 (s, 3H, OCH_3). Anal. C, H, N.

8-Benzyloxypyrazolo[5,1-*c*][1,2,4]benzotriazine 5-Oxide (29). From **7**[29] and benzyl alcohol, at 30 °C for 2 h. Yellow crystals. TLC eluent: toluene/ethyl acetate/acetic acid 8:2:1 v/v/v. ^{1}H NMR ($CDCl_3$) δ 8.50 (d, 1H, H-6), 8.11 (d, 1H, H-2), 7.85 (d, 1H, H-9), 7.45 (m, 5H, Ph), 7.21 (dd, 1H, H-7), 6.73 (d, 1H, H-3), 5.35 (s, 2H, CH_2). Anal. C, H, N.

3-Ethoxycarbonyl-8-benzyloxypyrazolo[5,1-*c*][1,2,4]benzotriazine 5-Oxide (30). From **4**[29] and benzyl alcohol, at 30 °C for 2 h. Yellow crystals. TLC eluent: toluene/ethyl acetate/acetic acid 8:2:1 v/v/v. ^{1}H NMR ($CDCl_3$) δ 8.53 (s, 1H, H-2), 8.49 (d, 1H, H-6), 7.84 (d, 1H, H-9), 7.45 (m, 5H, Ph), 7.30 (dd, 1H, H-7), 5.30 (s, 2H, CH_2), 4.50 (q, 2H, CH_2), 1.40 (t, 3H, CH_3). Anal. C, H, N.

General Procedure for the Synthesis of 33−36. Starting from 8-iodopyrazolo[5,1-*c*][1,2,4]benzotriazine 5-oxide (**31**),[26] and 3-ethoxycarbonyl-8-iodopyrazolo[5,1-*c*][1,2,4]benzotriazine 5-oxide (**32**),[25] (0.30 mmol) a Suzuki-coupling reaction was performed using suitable boronic acid to obtain derivatives **33**, **35**, and **36**. Tetrakis-(triphenylphosphine)palladium(0) (30 mg, 0.026 mmol) was added to a solution of **31**[26] or **32**[25] and THF anhydrous (5.0 mL); suitable boronic acids (0.62 mmol) in absolute ethanol and aqueous sodium carbonate (2M, 4 mL) were added and the reaction mixture was heated at reflux temperature until the starting material disappeared in TLC. The suspension was treated with water and the precipitate was filtered and recrystallized.

For synthesis of derivative **34**, 8-(2-phenylethyl)pyrazolo[5,1-*c*][1,2,4]benzotriazine 5-oxide, the starting material **31**[26] (0.50 mmol) was dissolved in 2 mL of THF and a suspension of $PdCl_2$(dppf) CH_2Cl_2 (36 mg, 0.045 mmol), 2-phenylethylboronic acid (75 mg, 0.50 mmol), and potassium carbonate (207 mg, 1.50 mmol) in THF (5 mL) was added. The reaction was stirred at reflux temperature for 18 h, then cooled at room temperature, diluted with water, and extracted twice with diethyl ether. The organic layers were dried and evaporated under vacuum, and the residue was purified by silica gel column chromatography (eluting with toluene/ethyl acetate 8:2) as fast runner band.

8-Phenylpyrazolo[5,1-*c*][1,2,4]benzotriazine 5-Oxide (33). From **31**[26] and phenyl boronic acid. Yellow crystals. TLC eluent: *i*-propyl ether/cyclohexane 8:3 v/v. ^{1}H NMR ($CDCl_3$) δ 8.62 (m, 2H, H-6 and H-9), 8.12 (d, 1H, H-2), 7.86 (dd, 1H, H-7), 7.80 (dd, 2H, H-2′ and H-6′ Ph), 7.55 (m, 3H, H-3′, H-4′, and H-5′ Ph), 6.80 (d, 1H, H-3). Anal. C, H, N.

8-(2-Phenylethyl)pyrazolo[5,1-*c*][1,2,4]benzotriazine 5-Oxide (34). From **31**[26] and 2-phenylethylboronic acid. Yellow crystals. TLC eluent: toluene/ethyl acetate 8:2 v/v. ^{1}H NMR ($CDCl_3$) δ 8.44 (d, 1H, H-6), 8.23 (d, 1H, H-9), 8.10 (d, 1H, H-2), 7.39 (dd, 1H, H-7), 7.28 (m, 5H, Ph), 6.76 (d, 1H, H-3), 3.21 (t, 2H, CH_2), 3.08 (t, 2H, CH_2). Anal. C, H, N.

8-(*trans*-2-Phenylvinyl)pyrazolo[5,1-*c*][1,2,4]benzotriazine 5-Oxide (35). From **31**[26] and *trans*-2-phenylvinylboronic acid. Yellow crystals. TLC eluent: *i*-propyl ether/cyclohexane 8:3 v/v. ^{1}H NMR ($CDCl_3$) δ 8.54 (d, 1H, H-6), 8.48 (d, 1H, H-9), 8.12 (d, 1H, H-2), 7.75 (dd, 1H, H-7), 7.62 (d, 2H, H-2′ and H-6′ Ph), 7.46 (m, 4H, H-3′, H-4′, h-5′ Ph, and 8-CH═), 7.26 (d, 1H, Ph−CH═), 6.78 (d, 1H, H-3). Anal. C, H, N.

3-Ethoxycarbonyl-8-phenylpyrazolo[5,1-*c*][1,2,4]benzotriazine 5-Oxide (36). From **32**[25] and phenyl boronic acid. Yellow crystals. TLC eluent: *i*-propyl ether/cyclohexane 8:3 v/v. ^{1}H NMR ($CDCl_3$) δ 8.64 (d, 1H, H-9). 8.63 (d, 1H, H-6). 8.56 (d, 1H, H-2). 7.95 (dd, 1H, H-7). 7.79 (dd, 2H, H-2′, and H-6′ Ph). 7.58 (m, 3H, H-3′, H-4′, and H-5′ Ph), 4.50 (q, 2H, CH_2), 1.50 (t, 3H, CH_3). Anal. C, H, N.

General Procedure for Synthesis of 3-Halogen Derivatives, 37−42. A solution of suitable 8-substituted pyrazolo[5,1-*c*]-[1,2,4]benzotriazine 5-oxide, **33**−**35** (0.50 mmol) in chloroform was added to iodine monochloride (ICl) (1:2) chloroform solution to obtain compounds **37**, **38**, and **40**; addition of *N*-iodosuccinimide (NIS) (100 mg) and a catalytic amount of benzoyl peroxide to a solution of **35** (0.50 mmol) in $CHCl_3$ gave compound **39**. From starting material **33** (0.50 mmol), addition of *N*-chlorosuccinimide (NCS) or of an excess of bromine (1.0 mL) yielded compounds **41** and **42**, respectively. The final solution, monitored by TLC, was evaporated to dryness and the crude residue was recrystallized by suitable solvent.

3-Iodo-8-phenylpyrazolo[5,1-*c*][1,2,4]benzotriazine 5-Oxide (37). From **33** and ICl. Yellow crystals. TLC eluent: *i*-propyl ether/cyclohexane 8:3 v/v. ^{1}H NMR ($CDCl_3$) δ 8.62 (d, 1H, H-6), 8.58 (d, 1H, H-9), 8.14 (s, 1H, H-2), 7.89 (dd, 1H, H-7), 7.79 (dd, 2H, H-2′, and H-6′ Ph), 7.56 (m, 3H, H-3′, H-4′, and H-5′ Ph). Anal. C, H, N.

3-Iodo-8-(2-phenylethyl)pyrazolo[5,1-*c*][1,2,4]benzotriazine 5-Oxide (38). From **34** and ICl. Yellow crystals. TLC eluent: chloroform. ^{1}H NMR ($CDCl_3$) δ 8.43 (d, 1H, H-6), 8.20 (d, 1H, H-9), 8.08 (s, 1H, H-2), 7.30 (m, 6H, H-7, and Ph), 3.15 (m, 4H, CH_2-CH_2). Anal. C, H, N.

3-Iodo-8-(*trans*-2-phenylvinyl)pyrazolo[5,1-*c*][1,2,4]benzotriazine 5-Oxide (39). From **35** and NIS. Yellow crystals. TLC eluent: *i*-propyl ether/cyclohexane 8:3 v/v. ^{1}H NMR ($CDCl_3$) δ 8.53 (d, 1H, H-6), 8.43 (d, 1H, H-9), 8.13 (s, 1H, H-2), 7.78 (dd, 1H, H-7), 7.62 (d, 2H, H-2′, and H-6′ Ph), 7.46 (m, 4H, H-3′, H-4′, h-5′ Ph, and 8-CH═), 7.26 (d, 1H, Ph−CH═). Anal. C, H, N.

3-Iodo-8-(1-chloro-2-iodo-2-phenylethyl)pyrazolo[5,1-*c*][1,2,4]-benzotriazine 5-Oxide (40). From **35** and ICl, at 30 °C for 2 h. Orange crystals. TLC eluent: *i*-propyl ether/cyclohexane 8:3 v/v. ^{1}H NMR ($CDCl_3$) δ 8.57 (d, 1H, H-6), 8.49 (d, 1H, H-9), 8.15 (s, 1H, H-2), 7.68 (dd, 1H, H-7), 7.48 (m, 5H, Ph), 5.37 (d, 1H, CHI), 5.28 (d, 1H, CHCl). Anal. C, H, N.

3-Chloro-8-phenylpyrazolo[5,1-*c*][1,2,4]benzotriazine 5-Oxide (41). From **33** and NCS. Yellow crystals. TLC eluent: *i*-propyl ether/cyclohexane 8:3 v/v. ^{1}H NMR ($CDCl_3$) δ 8.61 (d, 1H, H-6), 8.57 (d, 1H, H-9), 8.09 (s, 1H, H-2), 7.90 (dd, 1H, H-7), 7.79 (dd, 2H, H-2′, and H-6′ Ph), 7.55 (m, 3H, H-3′, H-4′, and H-5′ Ph). Anal. C, H, N.

3-Bromo-8-phenylpyrazolo[5,1-*c*][1,2,4]benzotriazine 5-Oxide (42). From **33** and bromine. Yellow crystals. TLC eluent: *i*-propyl ether/cyclohexane 8:3 v/v.; ^{1}H NMR ($CDCl_3$) δ 8.62 (d, 1H, H-6), 8.58 (d, 1H, H-9), 8.11 (s, 1H, H-2), 7.90 (dd, 1H, H-7), 7.78 (dd, 2H, H-2′, and H-6′ Ph), 7.55 (m, 3H, H-3′, H-4′, and H-5′ Ph). Anal. C, H, N.

3-Iodio-8-benzyloxypyrazolo[5,1-*c*][1,2,4]benzotriazine (11R). From starting material **11** (0.28 mmol) following a previously described procedure of reduction with triethyl phosphite (TEP, 3.0 mL) in toluene (10 mL)[36] at refluxing temperature for 8 h. Yellow crystals. TLC eluent: toluene/ethyl acetate 8:3 v/v. ^{1}H NMR ($CDCl_3$) δ 8.60 (d, 1H, H-6), 8.28 (s, 1H, H-2), 7.87 (d, 1H, H-9), 7.48 (m, 6H, Ph, and H-7), 5.38 (s, 2H, CH_2O). Anal. C, H, N.

Pharmacological Methods. The experiments were carried out in accordance with the Animal Protection Law of the Republic of Italy, DL no. 116/1992, based on the European Communities Council Directive of 24 November 1986 (86/609/EEC). All efforts were made to minimize animal suffering and to reduce the number of animals involved. Male CD-1 albino mice (22−24 g) and male Wistar rats (180−200 g) (Harlan Italy) were used. Twelve mice and three rats were housed per cage and fed a standard laboratory diet, with tap water ad libitum for 12 h/12 h light/dark cycles (lights on at 7:00). The cages were brought into the experimental room the day before the experiment for acclimatization purposes. All experiments were performed between 10:00 and 15:00.

Rota-Rod Test. The integrity of the animals' motor coordination was assessed using a rota-rod apparatus (Ugo Basile, Varese, Italy) at a rotating speed of 16 rpm The treatment was performed before the test. The numbers of falls from the rod in 30 s, after drug administration, were counted.

Hole-Board Test. The hole-board test was used to evaluate the effects of drugs on a mouse's explorative capacity and curiosity. Mice were placed individually on the board and left free to explore both panel and holes for 5 and 30 min after drug administration.

Light/Dark Box Test. The apparatus (50 cm long, 20 cm wide, and 20 cm high) consisted of two equal acrylic compartments, one dark and one light, illuminated by a 60 W bulb lamp and separated by a divider with a 10 cm × 3 cm opening at floor level. Each mouse was tested by placing it in the center of the lighted area, facing away from the dark one, and allowing it to explore the novel environment for 5 min. The number of transfers from one compartment to the other and the time spent in the illuminated side were measured. This test exploited the conflict between the animal's tendency to explore a new environment and its fear of bright light.

Pentylenetetrazole (PTZ)-Induced Seizure. PTZ (90 mg/kg sc) was injected 30 min after the administration of drugs. The

frequency of occurrence of clonic generalized convulsions was noted over a period of 30 min.

Passive-Avoidance Test. The test was performed according to the step-through method described by Jarvik.[37] The apparatus consisted of a two-compartment acrylic box with a lighted compartment connected to a darkened one by a guillotine door. As soon as the mouse entered the dark compartment, it received a thermal shock punishment. The latency times for entering the dark compartment were measured in the training test and after 24 h in the retention test. The maximum entry latency allowed in the training and retention sessions was, respectively, 60 and 180 s.

Ethanol-Induced Sleeping Time Test. Ethanol (4 g/kg ip) was injected 30 min after drug administration. The duration of a loss of the righting reflex was measured as the sleep time. If the mice slept more than 210 min, the end-point was recorded as 210 min.

Drugs. Diazepam (Valium 10) (Roche), flumazenil (Tocris Cookson Ltd., UK), and pentylenetetrazole (PTZ) (Sigma) were the drugs used. All drugs were dissolved in isotonic saline solution (NaCl 0.9%) and injected sc/ip. New compounds were administered by the po route and were suspended in 1% carboxymethylcellulose sodium salt and sonicated immediately before use. Drug concentrations were prepared in such a way that the necessary dose could be administered in a 10 mL/kg volume of carboxymethylcellulose (CMC) 1% by the po, ip, or sc routes.

Statistical Analysis. All experimental results are given as the mean ± SEM An analysis of variance, ANOVA, followed by Fisher's protected least significant difference procedure for post hoc comparison were used to verify significance between two means of behavioral results. Data were analyzed with the StatView software for Macintosh (1992). *P* values of less than 0.05 were considered significant.

Building of Pharmacophoric Map. The procedure to obtain the pharmacophoric map is outlined as follows:

(1) *Drawing* of ligand structures (42) (InsightII).
(2) *Geometry optimization* of structures (DISCOVER cff91).
(3) *Conformational research* (simulated annealing) (900 K)→ 200 conformation/molecule (DISCOVER cff91).
(4) *Identification* of pharamcophoric points (for all conformations).
(5) *Cluster of similar conformations*/each ligand rms < 1.
(6) *Building of geometric average conformation* by cluster conformations.
(7) *Research of common pharmacophoric* points on geometric average conformation.
(8) *Conformation alignment*: one for each cluster (the conformation most similar to geometric average conformation).

The most important steps for the building of the pharmacophoric map are explained briefly below:

Geometry Optimization of Structures. Geometry optimizations were achieved with the cff91 force field of DISCOVER module of the INSIGHT II program by applying the Conjugate Gradients algorithm with a convergence criterion of 0.001 kcal/mol.

Conformational Research (Simulated Annealing). Stochastic process by a simulated annealing procedure, in vacuum, was carried out.

The calculations were carried out with the DISCOVER module of the INSIGHTII program using CFF91 force field (consistent force field). A multiple-step procedure was used. The molecule was energetically minimized. The minimized system was used as initial structure for the subsequent molecular dynamics (MD) simulation. The structures were heated gradually to 900 K and cooled gradually, after 5 ps, until 300 K. Finally, the structure was energetically minimized. For every molecule, this procedure was repeated 200 times (therefore for every molecule 200 conformations were collected).

Pharmacophoric Point Identification. The following pharmacophoric points (Pp) were identified:

(a) Ring: the geometric center of atoms forming the aromatic moiety in the case of aromatic rings.
(b) Lipophilic: the geometric center calculated among clusters of lipophilic atoms. Lipophilic atoms are carbon atoms sp^2 and sp^3, sulfur atom, and halogen such as bromine and iodine.
(c) Acceptor: the Pp represents the point in which it is necessary to have the respective target atom (H) to form an efficient hydrogen bond with acceptor atoms (N and O).
(d) Donor: the Pp position represents the point in which it is necessary to have the target atom (N, O) to form an efficient hydrogen bond.

Cluster of Similar Conformations. Conformations for each molecule are collected in clusters based on the similarity of the Pp position. The rms value defines the similarity degree; the limit for the cluster is 1. The number of clusters that is sufficient to collect at least 50% of the conformations obtained from simulated annealing were considered for each molecule in the subsequent steps.

Research of Common Pharmacophoric Points on the Geometric Average Conformation. The best combination that contains the greatest number of Pp endowed with the best similarity among all the molecules was drawn out (four Pp). The similarity of the spatial position of Pp is calculated by the average (between all collected molecular conformation) of difference of distance between the internal "pharmacophoric points" couples. The similarity index was called distance difference sum square (DDSS).

For example, if the structure i and the structure j present a combination of four points (i_1, i_2, i_3 and i_4 and j_1, j_2, j_3, and j_4), the DDSS relative to structures i and j is calculated by the following formula, where d^i_{1-2} represents the average distance between the i_1 and i_2 etc. DDSS was calculated for all molecules.

$$\mathrm{DDSS_{ij}} = [\left(d^i_{1-2} - d^j_{1-2}\right)^2 + \left(d^i_{1-3} - d^j_{1-3}\right)^2 + \left(d^i_{1-4} - d^j_{1-4}\right)^2 + \left(d^i_{2-3} - d^j_{2-3}\right)^2 + \left(d^i_{2-4} - d^j_{2-4}\right)^2 + \left(d^i_{3-4} - d^j_{3-4}\right)^2]/6$$

The closer this value is to 0, the better the similarity will be.

Conformation Alignment. For each cluster, the conformation that was closest to the average conformation was selected. The selected conformations (one for each molecule) were aligned to minimize the rms among the four common Pp (Lp-1, HBp-1a,b, HBp-2) using a simplex procedure.

Supporting Information Available: Analytical data of final compounds. This material is available free of charge via the Internet at http://pubs.acs.org.

References

(1) Nutt, D. J. $GABA_A$ receptors: Subtypes, Regional Distribution, and Function. *J. Clin. Sleep Med.* **2006**, *2*, S7–11.
(2) Mohler, H. $GABA_A$ receptor diversity and pharmacology. *Cell Tissue Res.* **2006**, *326*, 505–516.
(3) Sieghart, W. $GABA_A$ receptors as target for different classes of drugs. *Drugs Future* **2006**, *31*, 685–694.
(4) Sieghart, W. Structure, Pharmacology and Function of $GABA_A$ Receptor subtypes. *Adv. Pharmacol.* **2006**, *54*, 231–263.
(5) Cooke, A. J.; Hamilton, N. M. alpha-Subunit selective modulators of GABAA receptor function as CNS therapeutics. *Expert Opin. Ther. Pat.* **2002**, *12*, 1491–1501.
(6) Whiting, P. J. GABA-A receptors: A viable target for novel anxiolytics?. *Curr. Opin. Pharmacol.* **2006**, *6*, 24–29.
(7) Mathiasen, L. S.; Rodgers, R. J.; Mirza, N. R. Comparative effects of nonselective and subtype-selective gamma-aminobutyric $acid_A$ receptor positive modulators in the rat-conditioned emotional response test. *Behav. Pharmacol.* **2007**, *18*, 191–203.

(8) Rudolph, U.; Mohler, H. GABA-based therapeutic approaches: GABAA receptor subtype functions. *Curr. Opin. Pharmacol*. **2006**, *6*, 1–6.
(9) McKernan, R. M.; Rosahl, T. W.; Reynolds, D. S.; Sur, C.; Wafford, K. A.; Atack, J. R.; Farrar, S.; Myers, J.; Cook, G.; Ferris, P.; Garrett, L.; Bristow, L.; Marshall, G.; Macaulay, A.; Brown, N.; Howell, O.; Moore, K. W.; Carling, R. W.; Street, L. J.; Castro, J. L.; Ragan, C. I.; Dawson, G. R.; Whiting, P. J. Sedative but not anxiolytic properties of benzodiazepine are mediated by the GABAA receptor a1 subtype. *Nat. Neurosci*. **2000**, *3*, 587–592.
(10) Rudolph, U.; Mohler, H. Analysis of $GABA_A$ receptor function and dissection of the pharmacology of benzodiazepines and general anesthetics through mouse genetics. *Annu. Rev. Pharmacol. Toxicol*. **2004**, *44*, 475–498.
(11) Ebert, B.; Wafford, K. A.; Deacon, S. Treating insomnia: current and investigational pharmacological approaches. *Pharmacol. Ther*. **2006**, *112*, 612–629.
(12) Basile, A. S.; Lippa, A. S.; Skolnick, P. GABAA receptor modulators as anxioselective anxiolytics. *Drug Discovery Today: Ther. Strategies* **2006**, *3*, 475–481.
(13) Dawson, G. R.; Maubach, K.; Collinson, N.; Cobain, M.; Everitt, B. J.; MacLeod, A. M.; Choudhury, H. I.; McDonald, L. M.; Pillai, G. V.; Rycroft, W.; Smith, A. J.; Sternfeld, F.; Tattersall, D.; Wafford, K. A.; Reynolds, D. S.; Seabrook, G.; Atack, J. R. An inverse agonist selective for alpha5 subunit-containing GABAA receptor enhances cognition. *J. Pharmacol. Exp. Ther*. **2006**, *316*, 1335–1345.
(14) Maubach, K. The $GABA_A$ receptor as potential target for the treatment of cognitive dysfunction. *Drugs Future* **2006**, *31*, 151–162.
(15) Mohler, H.; Fritschy, J. M.; Crestani, F.; Hensch, T.; Rudolph, U. Specific $GABA_A$ circuits in brain development and therapy. *Biochem. Pharmacol*. **2004**, *68*, 1685–1690.
(16) Mohler, H. Molecular regulation of cognitive functions and developmental plasticity: impact of GABAA receptors. *J. Neurochem*. **2007**, *102*, 1–12.
(17) Atack, J. R. $GABA_A$ Receptor Subtype-Selective Efficacy: TPA023, an α2/α3 Selective Nonsedating Anxiolytic and α5IA, an α5 Selective Cognition Enhancer. *CNS Neurosci. Ther*. **2008**, *14*, 25–35.
(18) Pirker, S.; Schwarzer, C.; Wieselthaler, A.; Sieghart, W.; Sperk, G. GABA(A) receptors: immunocytochemical distribution of 13 subunits in the adult rat brain. *Neuroscience* **2000**, *101*, 815–850.
(19) Yee, B. K.; Keist, R.; von Boehmer, L.; Studer, R.; Benke, D.; Hagenbuch, N.; Dong, Y.; Malenka, R. C.; Fritschy, J.-M.; Bluethmann, H.; Feldon, J.; Mohler, H.; Rudolph, U. A schizophrenia-related sensorimotor deficit links {alpha}3-containing GABAA receptors to a dopamine hyperfunction. *Proc. Natl. Acad. Sci. U. S.A*. **2005**, *102*, 17154–17159.
(20) Hauser, J.; Rudolph, U.; Keist, R.; Mohler, H.; Feldon, J.; Yee, B. K. Hippocampal alpha5 subunit-containing $GABA_A$ receptors modulate the expression of prepulse inhibition. *Mol. Psychiatry* **2005**, *10*, 201–207.
(21) Guidotti, A.; Auta, J.; Davis, J. M.; Dong, E.; Grayson, D. R.; Veldic, M.; Zhang, X.; Costa, E. GABAergic dysfunction in schizophrenia: new treatment strategies on the horizon. *Psychopharmacology* **2005**, *180*, 191–205.
(22) Hansch, C.; Leo, A.; Hoeckman, D. Exploring QSAR, Hydrophobic, Electronic, and Steric Constant; ACS Professional References Book; American Chemical Society: Washington, DC, 1995.
(23) Costanzo, A.; Guerrini, G.; Ciciani, G.; Bruni, F.; Selleri, S.; Costa, B.; Martini, C.; Lucacchini, A.; Malmberg-Aiello, P.; Ipponi, A. Benzodiazepine Receptor Ligands. 4. Synthesis and Pharmacological evaluation of 3-Heteroaryl-8-chloropyrazolo[5,1-*c*][1,2,4]-benzotriazine 5-Oxides. *J. Med. Chem*. **1999**, *42*, 2218–2226.
(24) Costanzo, A.; Guerrini, G.; Ciciani, G.; Bruni, F.; Costagli, C.; Selleri, S.; Besnard, F.; Costa, B.; Martini, C.; Malmberg-Aiello, P. Benzodiazepine receptor ligands. 7. Synthesis and Pharmacological evaluation of new 3-ester of the 8-chloropyrazolo[5,1-*c*]-[1,2,4]benzotriazine 5-oxide. 3-(2-Thienylmethoxycarbonyl)derivative: an anxioselective agents in rodents. *J. Med. Chem*. **2002**, *45*, 5710–5720.
(25) Guerrini, G.; Costanzo, A.; Ciciani, G.; Bruni, F.; Selleri, S.; Costagli, C.; Besnard, F.; Costa, B.; Martini, C.; De Siena, G.; Malmberg-Aiello, P. Benzodiazepine receptor ligands. 8: Synthesis and pharmacological evaluation of new pyrazolo[5,1-*c*]-[1,2,4]benzotriazine 5-oxide 3- and 8-disubstituted: high affinity ligands endowed with inverse-agonist pharmacological efficacy. *Bioorg. Med. Chem*. **2006**, *14*, 758–775.
(26) Guerrini, G.; Ciciani, G.; Cambi, G.; Bruni, F.; Selleri, S.; Besnard, F.; Montali, M.; Martini, C.; Ghelardini, C.; Galeotti, N.; Costanzo, A. Novel 3-iodo-8-ethoxypyrazolo[5,1-*c*][1,2,4]benzotriazine 5-oxide as promising lead for design of [alpha]5-inverse agonist useful tools for therapy of mnemonic damage. *Bioorg. Med. Chem*. **2007**, *15*, 2573–2586.
(27) Guerrini, G.; Ciciani, G.; Cambi, G.; Bruni, F.; Selleri, S.; Melani, F.; Montali, M.; Martini, C.; Ghelardini, C.; Norcini, M.; Costanzo, A. Novel 3-aroylpyrazolo[5,1-*c*][1,2,4]benzotriazine 5-oxides 8-substituted, ligands at GABAA/benzodiazepine receptor complex: synthesis, pharmacological and molecular modeling studies. *Bioorg. Med. Chem*. **2008**, *16*, 4471–4489.
(28) Costanzo, A.; Guerrini, G.; Ciciani, G.; Bruni, F.; Costagli, C.; Selleri, S.; Costa, B.; Martini, C.; Malmberg-Aiello, P. Synthesis and Pharmacological evaluation of 3-(2-furyl)- and 3-(3-furyl)-8-chloropyrazolo[5,1-*c*][1,2,4]benzotriazine 5-oxide new 3-heteroaryl substituted benzodiazepine receptor ligands. *Med. Chem. Res*. **2002**, *11*, 87–101.
(29) Costanzo, A.; Guerrini, G.; Bruni, F.; Selleri, S. Reactivity of 1-(2-Nitrophenyl)-5-Aminopyrazoles under Basic Conditions and Synthesis of New 3-, 7- and 8-Substituted pyrazolo[5,1-*c*]-[1,2,4]benzotriazine 5-Oxides as Benzodiazepine Receptor Ligands. *J. Heterocycl. Chem* **1994**, *31*, 1369–1376.
(30) Starks, M. C.; Liotta, C. Phase Transfer Catalysis, Principles and Techniques; Academic Press: London, 1978.
(31) Molander, G. A.; Yun, C.-S. Cross-coupling reactions of primary alkylboronic acids with aryl triflate and aryl halide. *Tetrahedron* **2002**, *58*, 1465–1470.
(32) Guerrini, G.; Costanzo, A.; Bruni, F.; Ciciani, G.; Selleri, S.; Gratteri, P.; Costa, B.; Martini, C.; Lucacchini, A. Benzodiazepine receptor ligands III. Synthesis and biological evaluation of 2- and/or 3-substituted pyrazolo[5,1-*c*][1,2,4]benzotriazine 5-oxides. *Il Farmaco* **1999**, *54*, 375–389.
(33) Zhang, W.; Koehler, K. F.; Zhang, P.; Cook, J. M. Development of a comprehensive pharmacophore model for benzodiazepine receptor. *Drug Des. Discovery* **1995**, *12*, 193–248.
(34) Xiaohui, H.; Zhang, C.; Cook, J. M. Model of the BzR binding site: correlation of data from site-directed mutagenesis and the pharmacophore/receptor model. *Med. Chem. Res*. **2001**, *10*, 269–308.
(35) Clayton, T.; Chen, J. L.; Ernst, M.; Richter, L.; Cromer, B. A.; Morton, C. J.; Ng, H.; Kaczorowski, C. C.; Helmstetter, F. J.; Furtmuller, R.; Ecker, G.; Parker, M. W.; Sieghart, W.; Cook, J. M. An Updated Unified Pharmacophore Model of the Benzodiazepine Binding Site on -Aminobutyric Acid Receptors: Correlation with Comparative Models. *Curr. Med. Chem*. **2007**, *14*, 2755–2775.
(36) Guerrini, G.; Costanzo, A.; Bruni, F.; Selleri, S.; Casilli, M. L.; Giusti, L.; Martini, C.; Lucacchini, A.; Malmberg Aiello, P.; Ipponi, A. Benzodiazepine receptor ligands. Synthesis and biological evaluation of 3-, 7-, and 8-substituted pyrazolo[5,1-*c*]-[1,2,4]benzotriazines and 5-oxide derivatives. *Eur. J. Med. Chem* **1996**, *31*, 259–272.
(37) Jarvik, M. E.; Kopp, R. An improved one-trial passive avoidance learning situation. *Psychol. Rep*. **1967**, *21*, 221–224.